Methods
of Soil Analysis

Field-Scale Apparent Soil Electrical Conductivity

Dennis L. Corwin* and Elia Scudiero

Soils are notoriously spatially heterogeneous and many soil properties are temporally variable. Spatial variability of soil properties has a profound influence on agricultural and environmental processes, such as plant–water–soil interactions, water flow, and solute transport, resulting in within-field plant yield variation and degradation of soil quality, to mention only a few. Field-scale mapping of spatial variability and monitoring of temporally dynamic soil properties is necessary for a variety of edaphic activities, such as soil surveys, reclamation, crop selection, site-specific management, and soil quality assessment. There are various approaches for characterizing soil spatial variability, but none of these has been as extensively investigated and is as reliable and cost effective as apparent soil electrical conductivity (EC_a) directed soil sampling. Geospatial measurements of EC_a are well suited for characterizing the spatial distribution of soil properties because they are reliable, quick, and easy to take with GPS-based mobilized EC_a measurement equipment. Directed soil sampling based on geo-referenced measurements of EC_a is a proven and robust means of characterizing the spatial variability of any soil property that influences EC_a, including sol salinity, water content, texture, bulk density, organic matter, and cation exchange capacity. It is the goal of this methodology paper to provide an overview of the characterization of soil spatial variability across multiple scales using EC_a–directed soil sampling with a focus on the field scale. Mobile EC_a equipment, protocols, guidelines, special considerations, data reliability tests, and strengths and limitations are presented for characterizing spatial and temporal variation in soil properties using EC_a–directed soil sampling.

Abbreviations: ANOCOVA, analysis of covariance; ρ_b, bulk density; CEC, cation exchange capacity; DPPC, dual pathway parallel conductance; EC_a, apparent soil electrical conductivity (dS m^{-1}); EC_e, electrical conductivity of the saturation extract (dS m^{-1}); EM_h, electromagnetic induction measurement in the horizontal coil configuration; EMI, electromagnetic induction; EM_v, electromagnetic induction measurement in the vertical coil configuration; ER, electrical resistivity; ERT, electrical resistivity tomography; ESAP, EC_e Sampling, Assessment, and Prediction; FSR, field-specific regression; GIS, geographic information systems; GPR, ground penetrating radar; GPS, global positioning system; IDW, inverse distance weighting; MMSD, minimization of the means of the shortest distances; MSSD, mean squared shortest distance; MWMSD, minimization of the weighted means of shortest distance; OLS, ordinary least square; OM, organic matter; PCA, principal components analysis; RSSD, response surface sampling design; SP, saturation percentage; SSA, spatial simulated annealing; TDR, time-domain reflectometry; θ, water content; UK, universal kriging.

BACKGROUND AND RATIONALE FOR EC_a–DIRECTED SOIL SAMPLING TO CHARACTERIZE SPATIAL VARIABILITY

All soil properties are spatially variable, and some are temporally variable as well (e.g., water content and salinity). The significance of within-field spatial variability of soil properties has been scientifically acknowledged and documented since the classic paper by Nielsen et al. (1973) concerning the variability of field-measured soil water properties. As an example, the complex spatial nature of soil salinity at the surface is depicted in Fig. 1. The complexity of soil variability makes soil mapping a formidable and onerous task.

The characterization of soil spatial variability is without question one of the most significant areas of concern in soil science because of its broad reaching influence on field- and landscape-scale processes related to agriculture and the environment, including solute transport, water flow, within-field variation in crop yield, and soil salinity accumulation, to mention just a few (Corwin and Lesch, 2013, 2014). There are a variety of methods for potentially characterizing soil spatial variability including ground penetrating radar (GPR), aerial photography, multi- and hyper-spectral imagery, time-domain reflectometry (TDR), and apparent soil electrical conductivity (EC_a). However, none of these approaches have been as extensively investigated as the use of EC_a (Corwin and Lesch, 2005a).

The geospatial measurement of EC_a (dS m^{-1}) using geophysical techniques such as electrical resistivity (ER) and electromagnetic induction (EMI) is a sensor technology that has played, and continues to play, a major role in addressing the issue

USDA-ARS, US Salinity Lab., 450 West Big Springs Road, Riverside, CA 92507-4617. *Corresponding author (Dennis.Corwin@ars.usda.gov).

Methods of Soil Analysis
2016, Vol. 1
doi:10.2136/methods-soil.2015.0038

Received 30 Nov. 2015.
Accepted 19 July 2016.

Fig. 1. Aerial view of a typical salt-affected field, showing the complex spatial patterns of salinity (source: Corwin and Lesch, 2013).

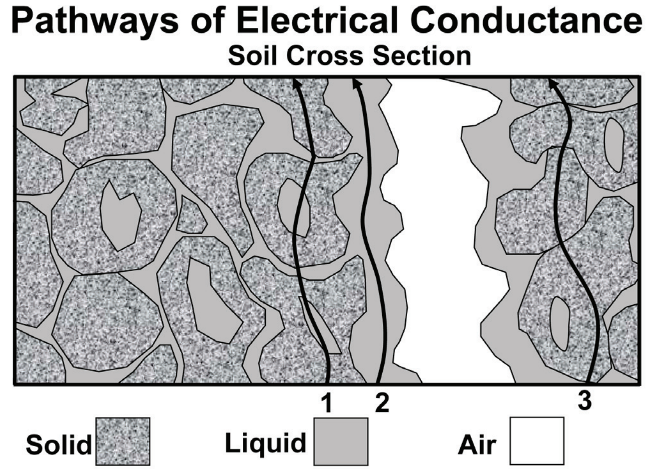

Fig. 2. Schematic illustrating the three conductance pathways for the apparent soil electrical conductivity (EC_a) measurement (modified from Rhoades et al., 1989). Pathway 1 is the solid–liquid conductance pathway, Pathway 2 is the liquid conductance pathway, and Pathway 3 is the solid conductance pathway.

of field-scale spatial variability characterization, particularly in mapping soil salinity, water content, and texture (Corwin and Lesch, 2005a; Doolittle and Brevik, 2014). Since its early agricultural use for measuring soil salinity, the application of EC_a has evolved into a widely accepted means of establishing the spatial variability of a variety of soil physical and chemical properties that either directly or indirectly influence the EC_a measurement (Corwin and Lesch 2003, 2005a; Corwin, 2005, 2008; Doolittle and Brevik, 2014). Scientists at the USDA-ARS US Salinity Laboratory have led the development of an integrated platform of mobilized ER and EMI equipment, software, and protocols for mapping soil spatial variability that has evolved into a standardized methodology (Corwin, 2008).

Apparent soil electrical conductivity is a measure of the bulk conductivity of the soil; that is, EC_a is a measure of anything conductive within the volume of measurement and is influenced, whether directly or indirectly, by any edaphic property that affects bulk soil conductance. Measurements of EC_a are complex because they reflect the influence of the interaction of several soil physical and chemical properties. This is a consequence of the fact that EC_a is a product of three parallel pathways of conductance, as illustrated in Fig. 2. The three parallel pathways of current flow that contribute to the EC_a measurement include: (i) a solid–liquid pathway (Pathway 1) primarily via exchangeable cations associated with clay minerals, (ii) a liquid phase pathway (Pathway 2) via salts contained in the soil water occupying the large pores, and (iii) a solid pathway (Pathway 3) via soil particles that are in direct and continuous contact with one another (Rhoades et al., 1989, 1999a).

Because of these pathways of conductance, EC_a is influenced by a complex interaction of salinity (i.e., EC_e, electrical conductivity of the saturation extract, dS m^{-1}), saturation percentage (SP), water content (θ), bulk density (ρ_b), organic matter (OM), cation exchange capacity (CEC), clay content and mineralogy, and temperature. The influences of salinity, water content, and temperature on electrical conductivity have been well known and documented (US Salinity Laboratory Staff, 1954). Saturation percentage and ρ_b are both directly influenced by OM and texture, particularly clay content in mineral soils (Stiven and Khan, 1966; Rhoades et al., 1990; Gavlak et al., 2003). Saturation percentage is especially reflective of the texture in mineral soils. The exchange surfaces on clays and OM provide a solid–liquid phase pathway primarily via exchangeable cations. Consequently, clay content (and mineralogy), CEC, and OM are recognized as factors influencing EC_a measurements. Measurements of EC_a *must* be interpreted with these interacting factors in mind.

The ability to measure a particular target property or properties with EC_a depends on the property or properties dominating the EC_a measurement at the specific site of measurement. For instance, consider the measurement of soil salinity by EC_a. To measure only soil salinity, the electrical conductance of only the soil solution (Pathway 2) is required. Since EC_a measures more than just soil salinity due to its three conductance pathways, the interpretation of the meaning of the EC_a measurement is complex. If salinity is sufficiently high (i.e., when EC_a is greater than 1–2 dS m^{-1}) to dominate the EC_a measurement, then other properties such as texture or water content may not be easily determined by EC_a, unless they happen to be correlated with salinity, which most often occurs when salinity is influenced and controlled in large part by the hydraulic regime created by texture. In essence, at high salinity levels the influence of salinity on the EC_a measurement dominates to the point where the influence of other soil properties (i.e., water content, texture, ρ_b, CEC, OM, mineralogy) becomes insignificant. In these instances, EC_a is essentially measuring only soil salinity. However, when salinity is low, and there is little significant influence of salinity on the EC_a measurement (i.e., $EC_a < 1$ dS m^{-1}), then the interpretation of the meaning of the EC_a measurement can only be established from ground-truth soil samples from which a relationship between EC_a and all potential soil properties influencing EC_a can be established. In an EC_a range of 1 to 2 dS m^{-1}, it is likely that several soil properties (e.g., salinity, water content, texture, bulk density) are influencing EC_a in a significant manner.

From a pore-scale perspective, electrolyte conduction through pores dominates over surface conduction when a high concentration of electrolyte occupies the pores. However, when the electrolyte concentration is dilute in the pore fluid, the effects of clay and surface conduction become important

(Boadu and Seabrook, 2006). The amount and distribution of clay, as well as the concentration of an electrolyte in the pore fluid, influence spectral electrical response measurements in a complex way that is not separable, but coupled (Boadu and Seabrook, 2006). It is the inseparable influence of soil properties on EC_a, particularly at $EC_a < 1$ to 2 dS m^{-1}, that causes the field-scale mapping of soil properties solely from geospatial EC_a measurements to be problematic, necessitating the collection of ground-truth soil samples to calibrate EC_a to those properties influencing EC_a at a particular site.

Even though the measurement of EC_a is complex, it is also reliable, easy to take, and easy to mobilize, making it a valuable mapping tool. An understanding and interpretation of geospatial EC_a data can only be obtained from ground-truth measurements of soil properties that correlate with EC_a from either a direct influence or indirect association. Due to its complexity and ease of mobilization, geospatial measurements of EC_a are used as a surrogate of soil spatial variability to direct soil sampling when mapping soil salinity or other target soil properties (e.g., texture, water content) at field scales and larger spatial extents. The approach for characterizing soil spatial variability from soil samples guided by variations in geospatial EC_a measurements is referred to as *EC_a–directed soil sampling*. Characterizing spatial variability with EC_a–directed soil sampling is based on the notion that when EC_a correlates with a soil property or properties, then spatial EC_a information can be used to identify sites that reflect the range and spatial variability of the property or properties (Corwin and Lesch, 2005b). These sites serve as soil sampling locations for ground truth to calibrate EC_a to the target property or properties.

The inseparable influences of the soil properties affecting EC_a is a complication that can be dealt with on a pedon scale using the models of Rhoades et al. (1990) and Lesch and Corwin (2003). At field scale, the effects are best separated out statistically on a field-by-field basis using soil samples obtained from an EC_a–directed soil sampling design to develop a field-specific model to calibrate EC_a to a target property, such as salinity, water content, or clay (Lesch et al., 2005). By adopting a direct calibration approach, one can optimally adjust for confounding soil property effects, while simultaneously obtaining an assessment of the accuracy and usefulness of the fitted model.

Numerous EC_a studies have been conducted that have revealed the site specificity and complexity of geospatial EC_a measurements with respect to the particular property or properties influencing the EC_a measurement at a study site. Corwin and Lesch (2003) point out the field specificity of geospatial EC_a measurements, which may be the consequence of geomorphological and anthropogenic factors. Corwin and Lesch (2005a, 2013) provided a compilation of EC_a studies and the associated edaphic property or properties that either directly or indirectly influence EC_a. These edaphic properties (and their earliest associated agricultural reference) include directly measured properties, such as salinity (Rhoades et al., 1976), water content (Rhoades et al., 1976), texture (Williams and Hoey, 1987), bulk density (Rhoades et al., 1999b), organic matter (Greenhouse and Slaine, 1983), and CEC (McBride et al., 1990), and indirectly measured properties, such as groundwater recharge (Cook and Kilty, 1992), heavy metals (Corwin and Ahmad, 2015), herbicide partition coefficients (Jaynes et al., 1995), leaching (Rhoades, 1981), pH (Bekele et al., 2005), soil map unit boundaries (Fenton and Lauterbach, 1999), and soil drainage classes (Kravchenko et al., 2002).

Table 1 provides a list of ground-based proximal sensor categories (i.e., sensors that take measurements from within a distance of 2 m from the soil surface) and the soil properties influencing each category of proximal sensor. Each sensor is typically affected by more than one agronomic soil property, with ER and EMI influenced by the most properties. To help understand and interpret complex geospatial EC_a measurement and to provide the full complement of spatial data needed to completely characterize not only edaphic but anthropogenic, topographic, meteorological, and biological properties that influence plant growth, multiple proximal sensors are recommended. For instance, Rodrigues et al. (2015) observed that the combined use of γ-ray spectrometry (e.g., as a proxy for texture) and apparent electrical conductivity (e.g., as a proxy for salinity) could be used to map all target soil properties and therefore understand and manage crop-yield spatial variability. In Italian coastal soils affected by saltwater intrusion, Scudiero et al. (2013) could model contrasting properties influencing crop yield only by combining measurements of apparent electrical conductivity (e.g., proxy for salinity) and bare-soil reflectance (e.g., proxy for organic carbon content).

In instances where EC_a correlates with a particular soil property, an EC_a–directed soil sampling approach will establish the spatial distribution of that property with an optimum number of site locations, which significantly reduces labor costs compared to grid sampling (Corwin et al., 2003a,b). Details for conducting a field-scale EC_a survey for the purpose of characterizing the soil spatial variability are in Corwin and Lesch (2005b). Protocols specifically for mapping soil salinity

Table 1. Soil properties influencing proximal sensors.†

	Agronomic soil property									
Category of proximal sensor	Texture (sand, silt, clay content)	OM	θ	EC or Na	Cp or ρ_b	Depth of topsoil or hard pan	pH	Residual NO_3 or total N	Other macronutrients	CEC
ER and EMI	X	X	X	X	X	X		X		X
Optical and radiometric	X	X	X				X	X		X
Mechanical					X	X				
Acoustic and pneumatic	X				X	X				
Electrochemical				X			X	X	X	

† Modified from Adamchuk et al. (2004). ER, electrical resistivity; EMI, electromagnetic induction; OM, soil organic matter; θ, water content; EC, electrical conductivity (salinity); Na, sodium content, Cp, compaction; ρ_b, bulk density, CEC, cation exchange capacity.

with EC_a–directed soil sampling are in Corwin and Lesch (2013).

Environmental and agricultural scientific literature is replete with studies that have failed to follow the guidelines and protocols first developed by Corwin and Lesch (2003, 2005b, 2013). Subsequently, there is extensive published research regarding the application of ER and EMI to map edaphic properties with dubious spatial data. Standards for conducting EC_a–directed soil sampling that will be widely adopted by those using ER or EMI to map edaphic properties are needed. The objective here is to provide an overview of the standardized methodology of field-scale characterization of soil spatial variability using EC_a–directed soil sampling by describing mobile EC_a equipment, protocols, guidelines, special considerations, tests for data reliability, and strengths and limitations.

MOBILIZED EC_a MEASUREMENT EQUIPMENT

Detailed descriptions of the theory, operation, and construction of ER and EMI instrumentation were provided by Rhoades et al. (1999a) and Hendrickx et al. (2002a). Mobilized EC_a–measurement equipment using ER or EMI instrumentation has been in use for more than two decades for the purpose of mapping and monitoring field-scale spatial soil salinity patterns (Rhoades, 1992, 1993; Corwin, 2008; Doolittle and Brevik, 2014). The design of a mobilized EC_a measurement system consists of four basic components: (i) EC_a measurement sensor, (ii) global positioning system (GPS), (iii) hardware interfacing, and (iv) transport platform.

Three types of EC_a measurement mobile sensors are available: (i) invasive four-electrode ER sensors, (ii) noninvasive EMI sensors, and (iii) TDR sensors. Invasive ER and noninvasive EMI sensors are the most popular sensors because the commercial development of a TDR sensor for use on a mobile apparatus has not progressed to a level where it is as efficient in operation as ER and EMI. Invasive four-electrode sensors can take the form of either insertion probes or surface arrays, with the latter being the configuration used for mobilized EC_a measurement systems. Examples of invasive ER four-electrode sensors configured as fixed-surface arrays include the equipment developed by Rhoades (1992, 1993) and Carter et al. (1993) and the commercial sensor technology used in the Veris 3100 system (Veris Technologies).[1] Commercial examples of EMI sensors include the Geonics EM-31, Geonics EM-38, DUALEM-1, DUALEM-2, DUALEM-21, and GF CMD-1 soil conductivity meters (Geonics Ltd., Dualem, GF Instruments), all of which can be easily mobilized. The DUALEM and GF equipment have the advantage of not requiring calibration. Comparisons between commercial EMI and ER equipment (Sudduth et al., 2003; Gebbers et al., 2009; Serrano et al., 2014) and between various commercial EMI sensors (Saey et al., 2009a; Urdanoz and Aragüés, 2012; Heil and Schmidhalter, 2015) are available in the literature.

There are two basic GPS systems that can be used in mobile EC_a–measurement equipment: (i) self-contained systems and (ii) stand-alone GPS receivers that require external data logging. The difference between the two is not in the GPS receiver technology, but in the interfacing. Self-contained GPS systems include data loggers and software programs that allow the user to record, modify, and/or store GPS coordinate data independent of attached sensors or hardware interfacing. Stand-alone GPS receivers typically must be connected to a microprocessor or electronic controller to store and/or process GPS coordinate data. The Trimble Pathfinder Pro-XRS and Trimble Ag132 GPS systems (Trimble) are examples of available commercial GPS systems.

Hardware interfacing is needed to link the EC_a measurement sensor data with associated GPS coordinate data and to control the timing of the data acquisition. The complexity of the hardware interface depends on the type and number of sensors and the extent of real-time data processing; consequently, the hardware interface tends to be system specific and expensive. However, in a simple mobile EC_a measurement system with a single electrical conductivity meter (i.e., single EM-38) the hardware interface can be omitted by direct output of real-time sensor data through an RS-232 serial connection with the data capture capability of the GPS system. The Veris system comes complete with interfacing and recording hardware, only requiring the user to plug in a compatible GPS receiver.

The final component of the mobile EC_a measurement system is the transport platform, which consists of either tow-able or self-mobilized platforms. The transport platform is optional since an EC_a survey can be conducted on foot with a basic EC_a system consisting of an EC_a sensor (ER or EMI), GPS, and data logger. Pickups, all-terrain vehicles, and tractors have been used as transport platforms to tow an EC_a sensor. The fixed-array four electrode (Rhoades, 1992, 1993) and Veris 3100 (Lund et al., 1999; Sudduth et al., 1999) are examples of ER sensor platforms that are towed. Simple nonmetallic platforms have also been developed to tow EMI instrumentation (Jaynes et al., 1993; Cannon et al., 1994; Kitchen et al., 1996; Freeland et al., 2002). An example of a self-mobilized platform includes a modified hydraulic-driven spray tractor with insertion-type, four-electrode EC_a sensors located on the rig's undercarriage that are driven into the ground with the hydraulic system, and a nonmetallic cylinder located at the front end that houses an EM-38, which is raised, lowered, and rotated 90° with the hydraulic system (Rhoades, 1992, 1993; Carter et al., 1993). In general, motorized platforms are more sophisticated, versatile, and expensive to develop than platforms that are towed behind a vehicle.

System integration can be dedicated or autonomous. In a dedicated system, all EC_a measurement sensors and GPS equipment are integrated directly into the transport platform. This system relies on extensive hardware interfacing and a central computer or controller to manage the data acquisition and data storage. In an autonomous system the GPS receiver and each EC_a measurement sensor can be easily removed from the platform and used independently. The Trimble Pathfinder Pro-XRS is an example of an autonomous system, whereas the Trimble Ag132 GPS is a dedicated system.

Surveys of EC_a to characterize soil spatial variability are used as spatial information to direct a soil sampling scheme that will provide the necessary ground-truth information to establish the spatial distribution of those soil properties correlated with EC_a within a field. For this reason, the inclusion of soil sampling equipment directly onto the platform is advantageous. The addition of soil sampling equipment allows the platform to serve as both an EC_a survey system and a soil

[1] All references to commercial equipment and instrumentation are provided solely for the benefit of the reader and does not imply the endorsement of the USDA.

sampling rig, which increases the versatility of the system. Figures 3 and 4 illustrate the components of a GPS-based mobile EC_a measurement system (Fig. 3a) developed at the US Salinity Laboratory. The system consists of a dual-dipole EM-38 that simultaneously measures vertical (EM_v) and horizontal (EM_h) electromagnetic induction EC_a (see Fig. 3b), a Giddings soil core sampler (Giddings Machine Co.) mounted on the front of the rig (see Fig. 3c), and a Trimble Pro-XL GPS system (see Fig. 4). The Trimble Pro-XL GPS system consists of a MC-V data logger, TANS receiver, battery pack, and dome antenna.

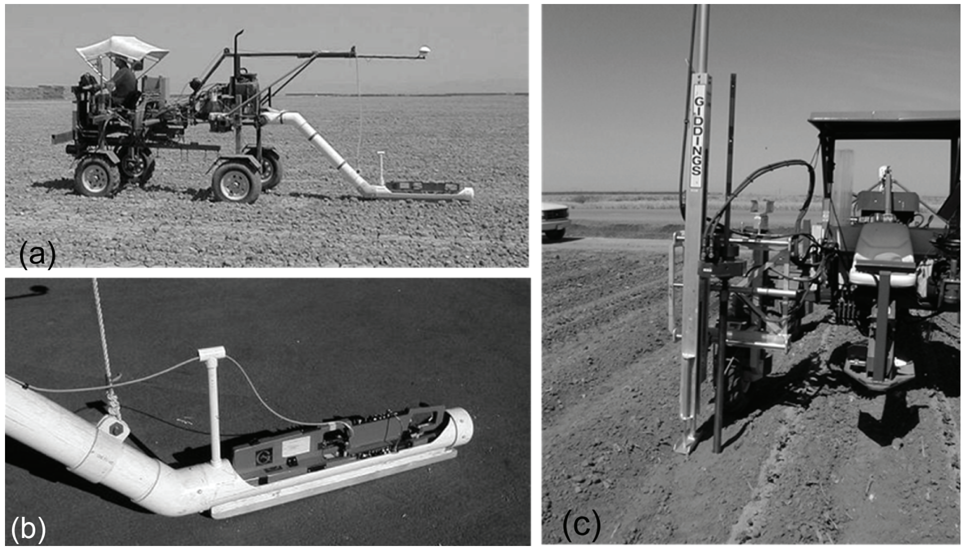

Fig. 3. Mobile electromagnetic induction equipment (source: Corwin and Lesch, 2005b): (a) complete rig; (b) close-up of sled holding the Geonics dual-dipole EM-38 soil electrical conductivity meter; and (c) close-up of Giddings soil core sampler.

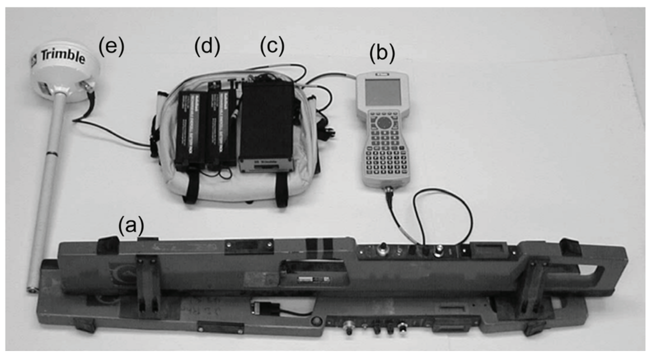

Fig. 4. Connection between (a) dual-dipole EM-38 soil electrical conductivity meter and Trimble MC-V Pro-XL system consisting of (b) MC-V data logger, (c) TANS receiver, (d) battery pack, and (e) dome antenna (source: Corwin and Lesch, 2005b).

The use of mobile EMI equipment has three advantages over the use of mobile ER equipment: (i) the ability to take measurements on dry and stony soils, (ii) the ability to traverse fields with growing crops, and (iii) the ability to traverse fields with beds and furrows. Under dry soil conditions, the physical contact needed between ER electrodes and soil for continuous electrical current flow is difficult to maintain. Stony soils are damaging to the ER electrodes. Crops and bed–furrow systems pose a problem for ER equipment, such as the Veris 3100, because of destruction of the crop and beds by the electrodes and soil–electrode contact problems on an uneven soil surface. The coulters or insertion probes of ER equipment are on a fixed-height or limited-height adjustable platform that cannot clear most crops, nor are they easily adjusted to conform to abrupt changes in microtopography as found in bed–furrow systems. In contrast, EMI equipment is designed so the platform clears most crop canopies and the EM-38 slides down furrows.

REVIEW OF PROCEDURE: PROTOCOLS, STRENGTHS, LIMITATIONS, AND INTERFERENCES

In instances where EC_a correlates with a particular soil property, an EC_a–directed soil sampling approach will establish the spatial distribution of that property with an optimum number of site locations to characterize the variability and keep labor costs minimal (Corwin et al., 2003b). Also, if EC_a is correlated with crop yield, then an EC_a–directed soil sampling approach can be used to identify those soil properties that are causing variability in crop yield (Corwin et al., 2003a). The purpose of an EC_a survey from a soil quality perspective is to establish the within field variation of soil properties that influence the field's intended use (e.g., agricultural productivity, environmental protection, wastewater recycling, etc.). The purpose of an EC_a survey from a site-specific crop management perspective is to establish the within-field variation of soil properties influencing the variation in crop yield (Corwin et al., 2003a; Corwin and Lesch, 2010).

Corwin and Lesch (2003, 2005b, 2013) developed protocols and guidelines for characterizing soil spatial variability from EC_a–directed soil sampling, with emphasis given to mapping soil salinity. A detailed discussion of each step in the protocols was provided by Corwin and Lesch (2005b, 2013). Table 2 presents a modification of the step-by-step protocols developed by Corwin and Lesch (2005b, 2013). The basic elements of a field-scale EC_a survey applied to soil quality assessment, monitoring of soil property changes, and site-specific crop management include (i) recording of metadata, site description, GPS control and boundary points, and EC_a survey objective; (ii) EC_a survey design; (iii) georeferenced EC_a data collection; (iv) soil sample design based on georeferenced EC_a data; (v) soil sample collection; (vi) physical and chemical analysis of pertinent soil properties; (vii) development of a stochastic and/or deterministic calibration of EC_a to a target property (e.g., soil salinity); (viii) spatial statistical analysis; (ix) geographic information system (GIS) database development; and (x) graphic display of spatial data.

The protocols to measure and map the spatial variability of a target soil property (e.g., salinity, water content, texture) at field scale are an effort to minimize soil property effects outside the target property of interest and to avoid the

Table 2. Apparent soil electrical conductivity (EC_a) protocols for mapping spatial variability.†

1. Metadata, site description, GPS, and EC_a survey objective
   a. Record metadata (e.g., equipment used, data format, date and time of data collection, etc.).
   b. Study site description: site location, soil survey information, presence or absence of vegetation, type of irrigation, topography, and surface condition.
   c. Select GPS coordinate system, establish control points and boundary points.
   d. Define the project's/survey's objective (e.g., inventorying, spatiotemporal monitoring, site-specific management, etc.).
   e. Establish the target property (i.e., the property to be mapped) or properties based on the project's objective.
2. EC_a survey design
   a. Establish EC_a measurement intensity (i.e., number and location of traverses and space between EC_a measurements with careful consideration of edge effects).
   b. Minimize secondary influences on EC_a (e.g., compaction, surface roughness and geometry, metal).
   c. Special EC_a survey design considerations
      (1.) presence of beds and furrows: perform separate surveys for the beds and for the furrows
      (2.) vineyards with metal trellising
         (a.) maximize distance from metal for surveys with electromagnetic induction (EMI)
         (b.) place an insulator between metal posts and trellis wires to break the conductance loop from the soil to the posts along the wires and back into the soil (this applies to both ER and EMI surveys)
      (3.) presence of drip lines: perform separate EC_a surveys over and between drip lines
      (4.) variations in surface geometry or roughness: perform separate surveys with separate sampling designs for each area differing in surface roughness or surface geometry (i.e., disked, beds and furrows, etc.)
      (5.) temporal studies
         (a.) reference all EC_a measurement to 25°C or
         (b.) conduct EC_a surveys at same time of day and same day of year
3. EC_a data collection with mobile GPS-based EC_a equipment (e.g., electrical resistivity or EMI)
   a. When using EMI, conduct drift runs to determine the effect of ambient temperature on EMI instrumentation.
   b. Georeference site boundaries and significant physical geographic features with GPS.
   c. Assure that water content at study site is at or near field capacity (≥70% field capacity) throughout the field (if water content is <70%, then do not conduct EC_a survey).
   d. Measure georeferenced EC_a data at the pre-determined spatial intensity and record associated metadata.
   e. Keep speed of mobile GPS-based equipment <10 km h^{-1} to reduce GPS positional errors.
4. Soil sample design based on geo-referenced EC_a data
   a. Statistically analyze EC_a data using an appropriate statistical sampling design (i.e., model- or design-based sampling design) to establish the soil sample site locations.
   b. Establish site locations, depth of sampling, sample depth increments, and number of cores per site (>100 soil samples are desirable but the total number of samples is largely determined by the resources available to analyze the soil properties of concern).
5. Soil core sampling at specified sites designated by the sample design
   a. Obtain measurements of soil temperature through the profile at selected sites.
   b. At randomly selected locations obtain duplicate soil cores within a 1-m distance of one another to establish local-scale variation of the target property (and other soil properties) for 20% or more of the sample locations.
   c. Record soil core observations (e.g., temperature, color, $CaCO_3$, gleying, organic matter, mottling, horizonation, textural discontinuities, etc.).
6. Laboratory analysis of target property and other EC_a–correlated soil properties relevant to the project objectives
7. Stochastic and/or deterministic calibration of EC_a to target property (and to other soil properties)
8. Spatial statistical analysis to determine the soil properties influencing EC_a
   a. Perform a basic statistical analysis of the target property (and other relevant soil properties) by depth increment and by composite depth over the depth of measurement of EC_a.
   b. Determine the correlation between EC_a and target property (and between EC_a and other soil properties) by composite depth over the depth of measurement of EC_a.
9. GIS database development
10. Graphic display of spatial distribution of target property (and other properties correlated to EC_a) using various interpolation methods (e.g., inverse distance weighting, cubic spline, geostatistics)

† Modified from Corwin and Lesch (2005b, 2013). EMI, electromagnetic induction; GIS, geographic information system; GPS, global positioning system.

confounding influence of soil condition effects. This is represented schematically in Fig. 5, where soil property effects (e.g., soil temperature, water content, texture, bulk density, and OM) are primary influences on the EC_a measurement, and soil condition effects are secondary influences when considering soil salinity as the target property. Soil property effects include any soil property influencing EC_a other than the target property, while soil condition effects are influences such as metal, surface roughness, soil compaction, and surface geometry (e.g., presence of beds and furrows). Accurate maps of the target property will not be obtained using EC_a–directed sampling unless the primary influences are understood and the secondary influences are minimized.

The protocols for EC_a–directed soil sampling are applicable to both nonsaline (i.e., EC_e <4 dS m^{-1}, which roughly corresponds to an EC_a <0.5 to 1 dS m^{-1}, depending on the texture) and saline (i.e., EC_e >4 dS m^{-1}, which corresponds to an EC_a >0.5 to 1 dS m^{-1}, depending on the texture) soils. However, salinity, particularly in saline soils, will tend to dominate the EC_a measurement, masking the influence of other soil properties influencing bulk soil conductance. This creates greater difficulty in characterizing the spatial patterns of water content,

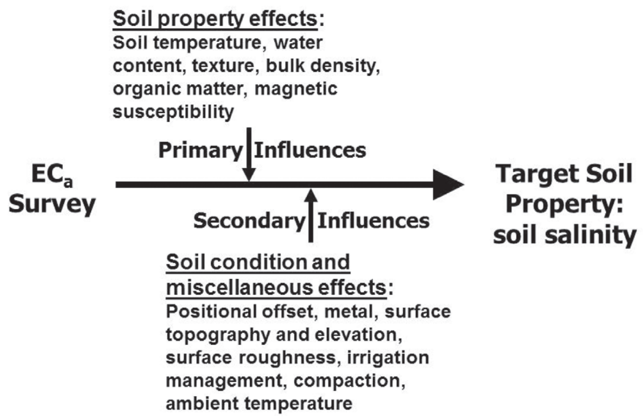

Fig. 5. Conceptual path diagram of the primary and secondary factors influencing an apparent soil electrical conductivity (EC$_a$) survey targeted at measuring soil salinity (source: modified from Corwin and Lesch, 2013).

texture, OM, etc., except when these properties correlate with salinity. In contrast, salinity in nonsaline soils (or more specifically where EC$_a$ is below about 1 dS m^{-1}) no longer has an overriding influence. Therefore, properties like water content, texture, OM, and others are more easily modeled using a field-specific model that calibrates the target property to EC$_a$.

The protocols also apply to both nonirrigated (i.e., dryland farming) and irrigated fields. However, issues related to adequate water content (i.e., water content at or near field capacity) are generally less of a concern for irrigated fields than dryland fields because regular irrigation maintains water content at optimal levels. Greater awareness should be given to water content levels on dryland fields when conducting an EC$_a$ survey.

The goal of the protocols is to mitigate the influence of variations in surface geometry (flat vs. beds–furrows), surface roughness (disked vs. smooth), temperature (both soil temperature effects and ambient temperature effects on the instrumentation), water content, compaction, edge effects, and textural discontinuity to assure reliable, accurate EC$_a$ survey data. Failure to follow the EC$_a$–directed soil sampling protocols will likely render spurious, unreliable EC$_a$ measurements, resulting in inaccurate calibration of EC$_a$ to the target property and erroneous maps of the target property or properties.

INDIVIDUAL STEPS IN THE ANALYSIS

Step 1: Metadata, Site Description, GPS, and EC$_a$ Survey Objective

Record the metadata (e.g., equipment used to collect data, data format and organization, date of data collection), descriptive information for the study site (e.g., climate, vegetation, general geographic features), and relevant GPS information, including: (i) general site location, (ii) GPS coordinate system used, (iii) control points, (iv) GPS boundary points, (v) soil survey information (e.g., soil type), (vi) presence or absence of vegetation, (vii) type of irrigation (i.e., natural rainfall, sprinkler, drip, flood), (viii) topography, and (ix) surface conditions (e.g., smooth, disked, beds–furrows).

Once metadata and basic descriptive site information have been collected, establish the objective of the EC$_a$–direct soil sampling survey. For example, is the objective of the survey to inventory and/or monitor soil quality, to establish within-field variation in soil properties influencing plant yield, to serve as ground truth for a regional-scale assessment of a target property, or some other purpose? The survey's objective must be defined based on the project goals and available resources (e.g., personnel, funding, analytical capabilities).

Step 2: EC$_a$ Survey Design

The EC$_a$ measurement intensity and survey design, which includes the number and location of traverses and space between the EC$_a$ measurements, is based on the EC$_a$ survey objective. Measurement intensities generally vary from every 3 to 5 m between measurement locations for intense surveys used in detailed field-scale studies to 75 to 100 m for landscape-scale studies of thousands or tens of thousands of hectares. Typically, an 18-ha field can be surveyed with mobile EC$_a$ equipment in one to two 8-h work days at a 5-m spacing, which results in roughly 7200 locations where EC$_a$ measurements are taken. This level of survey intensity provides a map of spatial variation sufficiently detailed to meet most intended purposes. If the EC$_a$ survey is used for site-specific management, then measurements taken every 5 m are appropriate (see Corwin et al., 2003a), whereas if the EC$_a$ survey is used for the calibration of remote imagery for a regional-scale assessment of salinity, then 10 traverses with measurements taken 15 to 30 m (or farther) apart within a 30-ha field will suffice (see Lobell et al., 2010).

The EC$_a$ survey design should focus on minimizing the confounding effects that secondary influences (see Fig. 5) have on obtaining reliable EC$_a$ data. These secondary influences include positional offset effects, field edge effects, metal, surface topography and elevation, surface roughness, irrigation management, compaction due to farm vehicles, and ambient temperature effects on instrumentation.

The issue of positional accuracy in EMI measurements of EC$_a$ for precision agriculture was addressed by Sudduth et al. (2001). Positional offset can be a problem due to both the distance from the sensor to the GPS antenna and the data acquisition system time lags. Sudduth et al. (2001) found that the sensitivity of EC$_a$ to variations in sensor operating speed and height was relatively minor. Nevertheless, mobile EC$_a$ equipment should not be operated at speeds higher than 10 km h^{-1} to minimize positional offset effects.

The EC$_a$ survey should be designed to avoid field edge effects; that is, a buffer area around the edge of the field should be made where no EC$_a$ measurements are taken. This is particularly important for EC$_a$ surveys that characterize the spatial distribution of dynamic soil properties, such as salinity and water content. This will eliminate the possibility of the selection of sampling sites near the field's edge, which are areas where unrepresentative extremes may occur. Edge effects can be the consequence of a variety of processes and are common to agricultural fields where the boundary of the field has a sharp transition, and the anthropogenic, meteorological, biological, and edaphic factors influencing plants (or animals) are not representative of the field as a whole. As an example, runoff from roads surrounding a field can cause increased leaching of salts and higher water contents at the edges of fields. Salts used to de-ice roads at the edge of fields can accumulate. Higher temperatures and lower relative humidity at the edges of a field can cause increased evapotranspiration, which reduces leaching and lowers water contents, thereby increasing salinity. These and other processes can result in salinity and water content levels at the edges of fields that are not representative and do not reflect the processes occurring throughout the rest of the field; consequently, a buffer area around the field is recommended where no EC_a measurements are taken so the sampling design is not influenced by unrepresentative edge effects.

The issue of edge effects influencing the sampling design is of particular concern for the response surface sampling design used in the ESAP (EC_e, Sampling, Assessment, and Prediction) software developed at the US Salinity Laboratory by Lesch et al. (2000) because the software identifies sampling sites by minimizing clustering, which often results in the identification of sites near the edge. To combat the influence of edge effects, ESAP has a built-in means of creating a buffer area at the edge of a field where EC_a measurements can be omitted.

As a rule-of-thumb for a rectangular field, the first and last traverses and the start and end of each traverse using mobile georeferenced EC_a equipment should be a distance of $0.5(w/n)$ and $0.5(d/n)$, respectively, from the edge of the field to avoid edge effects (the distance between traverses is d/n), where w is the width of the field, d is the length of the field, and n is the number of desired EC_a traverses. For nonrectangular fields, the first and last traverses and the start and end of each traverse can be $0.5(w/n)$ from the edge of the field, where w is now the greatest width of the field. This rule-of-thumb is of greatest importance when a small number of soil sample sites are selected (e.g., <10), whether by a model- or designed-based sampling strategy, from a minimal number of traverses (e.g., <10). Concern for edge effects becomes less of an issue as the number of traverses and soil sample sites increases. When large numbers of traverses are taken, edge effects do not disproportionately influence the sampling design, but when few traverses are taken, the sampling design is unduly influenced by less representative EC_a values that are the result of processes confined mainly to the edge of the field.

The influence of metal on the EC_a measurement is a concern at all times. This includes metal fences, vineyard trellises, buried metal objects, and underground metal pipe. Metal should be kept outside the volume of measurement whether for ER or EMI. Metal is particularly a concern for EC_a surveys of vineyards with metal trellises. Metal trellises in vineyards pose a challenge to EC_a surveys, both for EMI and for ER. Use of EMI for surveys of EC_a within vineyards with metal trellising have shown that the metal trellis distorts the EC_a values, causing increases as high as 0.50 dS m^{-1} or more (Lamb et al., 2005). Close attention needs to be given to take EMI measurements of EC_a sufficiently far from any metal post and trellis wires to eliminate any magnetic influence on the EMI conductivity reading. An EC_a survey of a vineyard with metal trellises should take the metal posts and wires of the trellises into account by positioning the EM-38 midway between surrounding metal posts and keeping the EM-38 at ground level away from the trellis. Corwin and Lesch (2013) found that when the trellises were ignored and EMI measurements were taken without regard for the position of nearby metal posts, the average EM_h and EM_v were roughly 0.10 dS m^{-1} higher, which are spurious elevated results due to the influence of metal. When trellises in a vineyard are comprised of steel posts, Lamb et al. (2005) recommended that EMI surveys should only be conducted where the row spacing is 3 m or more and traverses are made mid-row.

Corwin and Lesch (2013) also found that there is not only a magnetic influence by the metal trellises, but that there is a continuous conductance loop that extends from the soil up through the metal post, along the trellis, back down the adjacent metal post, and returning into the soil. This conductance loop is measured with both EMI and ER; therefore, the influence of metal trellises is not solely a magnetic effect that only influences EMI and not ER. The fact that ER is not affected by magnetic influences caused by the presence of metal does not mean it is automatically the instrument of choice for vineyards with metal trellises. To remove the influence of metal on either ER or EMI, the conductance loop can be broken by inserting an insulator between the metal posts and trellis wires. For numerous georeferenced EC_a measurements, the insertion of an insulator between all trellis wires and supporting posts is likely impractical. However, as long as the trellis system configuration (i.e., spacing of posts, dripper guide-wire, and cordon, gripper, and foliage wires) remains the same and measurements are taken in the same position relative to the trellis, the metal influences the absolute EC_a values in a way that can be characterized similarly to "background noise" and in most instances can be disregarded.

Surface topography plays a significant role in influencing spatial EC_a variation. Slope and aspect will influence OM content and will determine the level and location of runoff and infiltration, which will influence the variation in water content and salinity at local scales and larger (Hanna et al., 1982). Areas where the slope is steep tend to have lower water content than areas where a depression occurs. All other factors being equal, flat areas tend to be more spatially uniform in areal variation of water content. The influence of surface topography on salinity distribution coincides with the influence of surface topography on water flow gradients, which result in salt transport.

The bed–furrow environment is an example of surface topography that can have subtle local-scale variation effects. The bed–furrow topography can be a source of considerable water and salinity variation, particularly over the cropping season. Flood irrigation down furrows causes a percentage of the irrigation water applied to move laterally and upward into adjacent beds due to capillary flow. This water movement will carry near-surface soluble salts up into the bed, resulting in a complex distribution of salinity within the furrow. The presence of beds and furrows and drip irrigation requires special EC_a survey considerations because of the abrupt changes that occur in water content and salt accumulation. To get a comprehensive understanding of the salinity distribution, separate EC_a surveys are needed for the furrow and for the bed. Similarly, abrupt changes in water content and salinity distribution occur under drip irrigation. To get a more realistic understanding of soil salinity distribution in fields under drip irrigation, field-scale EC_a surveys should be conducted so that traverses are made within and between drip lines. Figure 6 shows the dramatic difference in the spatial patterns and magnitude of EC_a as measured with EM_h for in-row and between-row traverses of the drip-irrigated vineyard in Napa Valley, California. The in-row average EC_a (EM_h = 0.75 dS m^{-1}) is higher than the between-row average EC_a (EM_h = 0.52 dS

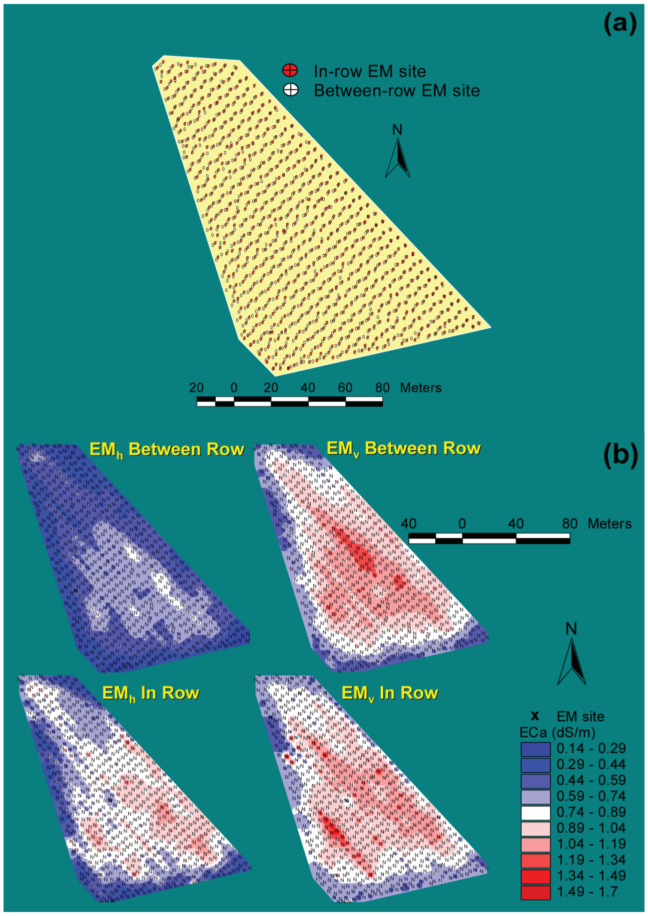

Fig. 6. Napa Valley (Caneros Region) apparent soil electrical conductivity (EC_a) survey of a vineyard using electromagnetic induction (EMI): (a) site locations and (b) EM_h and EM_v measurements between and in row, where EM_h and EM_v are the EMI measurements in the horizontal and vertical coil configurations (source: Corwin and Lesch, 2013).

m^{-1}) because of the higher water content below the drip lines. The complex three-dimensional nature of salt and water distribution under drip irrigation cannot be understood without surveying both within and between drip lines to avoid misinterpretation of the spatial EC_a information concerning water content and soil salinity.

More extensive sampling schemes must be considered for bed–furrow and drip-irrigation systems if knowledge of the two-dimensional salinity and/or water content distributions is an essential objective of the survey. However, if a detailed knowledge of the two-dimensional distributions of a bed–furrow or drip-irrigation system is unnecessary, then consistency with respect to soil core locations is essential. In these instances, all soil cores should be sampled from the same place within the bed–furrow or with respect to the drip line. Furthermore, the EC_a survey data, particularly when using EMI equipment, and soil sample cores should be acquired from exactly the same location within the bed–furrow or with respect to the drip line. More specifically, if EC_a data are acquired from the furrows, then soil samples should also be acquired from the furrows; if EC_a data are acquired from the beds, then soil samples should also be acquired from the beds; if EC_a data are acquired in the drip line, then soil samples should be acquired in the same location.

When evaluating the influence of a target soil property on crop growth and yield, composite sampling strategies for averaging lateral variations in a bed–furrow or drip-irrigation system should be used with caution (Corwin and Lesch, 2005b). In composite sampling, soil samples would be acquired from both bed and furrow locations (or along and between the drip lines) and then mixed together in an effort to obtain a more "representative" sample of the root zone. There are three reasons for exercising caution when using composite samples for averaging lateral variations. First, it doubles the field work without providing any knowledge of the two-dimensional, bed–furrow (or drip system) salinity distribution. Second, it often introduces more variability into the sample data through poor soil-mixing processes than it removes through averaging. Third, it may not be representative of the root zone.

Irrigated agricultural land is typically laser-leveled to improve irrigation efficiency. Various leveling designs are used depending on the method of irrigation and the agricultural crop under production. The three most common designs include dead leveling, single-slope leveling, and dual slope leveling. All these three designs create a theoretical plane that can be written mathematically as:

$$SE = \alpha_0 + \alpha_1 x + \alpha_2 y \qquad [1]$$

where SE represents the surface elevation, x and y represent the physical (x, y) coordinates, and the α_0, α_1, and α_2 are the coefficients, with α_1 and α_2 representing the primary and secondary slopes of the field, respectively. Equation [1] is referred to as a first-order trend surface equation. The regression relationship between the georeferenced EC_a measurements and soil properties (i.e., salinity, water content, texture) influencing the EC_a measurement can be influenced by gradual changes in salinity, water content, and/or texture across the survey area due to changes in elevation. These gradual changes in salinity, water content, and/or texture due to elevation can be taken into account through the inclusion of a first-order or second-order trend surface equation in the regression analysis.

If an EC_a survey is conducted on non-graded farmland, which exhibits significant local variation in surface elevation, then it will usually be necessary to conduct a surface elevation survey along with the EC_a survey. The elevation data can then be directly incorporated into any regression analyses relating EC_a to soil properties or into the sample design strategy.

The EC_a survey design must also consider surface roughness (i.e., smooth or disked surface) and surface geometry (i.e., presence and absence of beds and furrow). As an example, Fig. 7 shows an EMI survey of EC_a (i.e., EM_h) of a field where the northern end was disked flat and the southern end was in beds and furrows. As can be seen, there is a sharp boundary between the flat disked area and bed–furrow area, showing the influence of the presence of beds and furrows, which is a result of salt accumulation in the beds caused by the lateral and upward flow of leached salts from the furrow into the bed. The roughness of the soil surface can also influence spatial EC_a measurements. Geospatial EC_a measurements taken on a smooth field surface will be higher than the same field with a rough surface from disking. This is because the disturbed disked soil acts as an insulating layer to the conductance

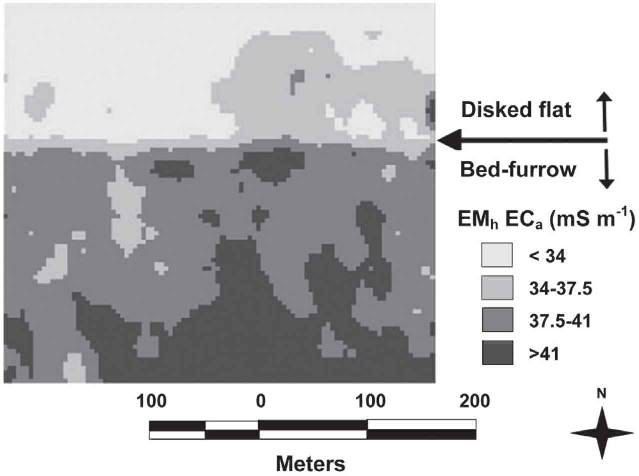

Fig. 7. Effect of the presence of beds and furrows on apparent soil electrical conductivity (EC_a) measurements when using electromagnetic induction taken in the horizontal coil configuration (EM_h) (source: Corwin and Lesch, 2013).

pathways, thereby reducing its conductance (Corwin and Lesch, 2013). The extent of the reduction in conductance depends on the depth of the plow layer and the coarseness of the clods. When conducting a geospatial EC_a survey of a field, the entire field must have the same surface roughness and same surface geometry. If this is not the case, then separate EC_a surveys should be conducted for areas of different surface roughness, and sample sites should be selected separately.

Irrigation management has a pronounced effect on determining areal and profile EC_a distributions within a field. The amount and frequency of irrigation will directly influence the movement of water and soluble salts through the profile and across the field. The water content of the soil during the EC_a survey will be at least partially determined by the elapsed time from the last irrigation event, the presence or absence of a crop, and if present, the maturity of the crop. Dryland soils are particularly problematic because there may not be sufficient moisture within the entire soil profile to provide conductance through the liquid pathway (Pathway 2), which is necessary for an accurate EC_a measurement.

Since a change in irrigation management (e.g., drip, sprinkler, or flood irrigation) can seriously affect the three-dimensional salinity and water content distributions within a field, it is important to avoid conducting an EC_a survey (and/or soil sampling) for an area under more than one irrigation management strategy. This means that any survey area must be restricted to an area with the same irrigation management. Each survey must be conducted entirely within a single, homogeneous irrigation management area. The failure to restrict EMI readings to an area under a single water management strategy can result in serious regression model and sample design bias with inflated errors that corrupt the entire surveying process.

Another source of potential EC_a variation arises from soil compaction caused by repetitive traffic patterns of heavy agricultural equipment (Brevik and Fenton, 2004; Corwin and Lesch, 2005b) or by puddling in paddy rice (*Oryza sativa* L.) fields (Islam et al., 2014). In many fields, heavy equipment is consistently driven down the same set of furrows when performing tillage and cultivation operations over the growing season. This leads to a systematic pattern of compaction in a subset of furrows throughout the field. Figure 8 displays the EM-38 horizontal (EM_h) readings acquired in 1991 along 30 adjacent furrows in a buried drip-irrigated cotton (*Gossypium hirsutum* L.) field (Westlands Water District, California) subject to repetitive traffic influences. In this case the traffic pattern induced a clearly cyclic pattern in the EM_h readings; the highest conductivity readings consistently occurred in the compacted furrows, where ρ_b was characteristically higher near the soil surface. The data shown in Fig. 8 are atypical. In general, compaction induced cyclic patterns do not have such pronounced effects on EC_a. Nonetheless, caution should be taken to systematically avoid taking EC_a measurements down compacted furrows, particularly with EMI equipment. Excessive soil compaction will nearly always have at least some effect on the ρ_b, soil salinity, and water content levels. Random surveying (and sampling) of both compacted and noncompacted furrows in the same field will introduce variability that should be avoided whenever possible. A simple, but effective, means of determining furrows that have been compacted by repeated traffic from heavy equipment is by pushing a long screwdriver or rod into the furrow to determine if the resistance is greater than adjacent furrows. Islam et al. (2014) used a floating soil sensor system with the EM-38 EMI sensor to detect soil heterogeneity linked to soil compaction, which was useful for precision puddling and land preparation in paddy rice fields.

Ambient temperature changes can have an effect on the EMI instrumentation resulting in shifts in EC_a measurements during the course of the day. Changes in ambient temperature during the day cause the EMI sensor to drift, which can contribute to within-field EC_a variation. A study by Robinson et al. (2004) indicated that the drift commonly observed in the EM-38 is likely due to temperature effects on the EM-38 sensor and that a simple reflective shade over the sensor could reduce drift effects considerably. However, an added precaution would be to conduct regular "drift runs," where EC_a data are periodically acquired throughout the day along the same transect to adjust for the drift in the post-processing of EC_a data. Drift runs are generally conducted in the morning, noon, and late afternoon to provide a range of diurnal temperature

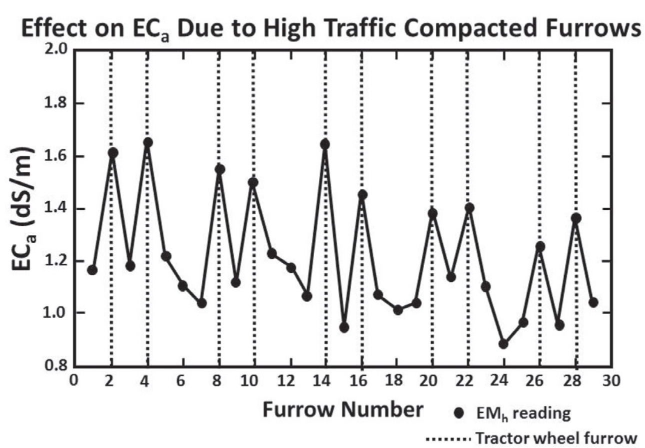

Fig. 8. Variations of apparent soil electrical conductivity (EC_a) due to compaction from repeated heavy equipment operation (source: Corwin and Lesch, 2005b).

effects on the EMI instrument. The variations in drift provide the basis for adjusting the EC_a measurements. As a rule-of-thumb, normalization of EC_a data using the drift runs should occur when successive drift runs are shifted by 5% or more. Another means of minimizing the effect of temperature is frequent nulling of the I/P reading (Brevik et al., 2004).

The above factors, if not taken into account when conducting an EC_a survey, will likely produce a "banding" effect. For example, if an EC_a survey is conducted on a field that has spatial and temporal differences in water content, soil profile temperature, surface roughness, and surface geometry, then bands of EC_a such as those found in Fig. 9 will result. These bands reflect the primary and secondary influences of soil moisture, soil temperature, surface roughness, and surface geometry that must be minimized to produce a reliable EC_a survey that can be used to direct soil sampling to spatially characterize the distribution of the target property, which in Fig. 9 is salinity.

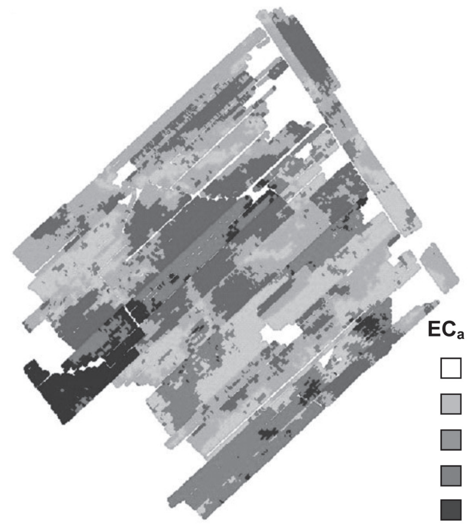

Fig. 9. Illustration of the "banding effect," which is characteristic of a failed apparent soil electrical conductivity (EC_a) survey of soil salinity, resulting from the disregard of primary (e.g., water content, bulk density, temperature, texture) and secondary influences (e.g., surface roughness, presence of beds and furrows, compaction due to heavy equipment) effecting EC_a (source: Corwin and Lesch, 2013).

Step 3: EC_a Data Collection with Mobile GPS-Based Equipment

There are a number of issues to consider in an EC_a survey that may have subtle or pronounced effects on the accuracy and reliability of the EC_a measurements. These effects relate to primary factors (see Fig. 5) that are easily overlooked, but may collectively mean the difference between useful and unreliable data.

Factors Influencing Reliability of EC_a Measurements

Variation of EC_a within a field is due to spatial variation in soil properties influencing EC_a. The spatial heterogeneity of these soil properties is the consequence of the interaction of (i) soil formation processes, (ii) meteorological processes, and (iii) anthropogenic influences. Soil formation processes are the result of complex interactions between biological, physical, and chemical mechanisms acting on a parent material over time and influenced by topography. Meteorological processes directly and indirectly influence soil formation processes. Anthropogenic influences are typically related to management practices, including crop selection, seed density, irrigation method (e.g., drip, sprinkler, flood), leaching fraction, and irrigation water quality. To implement an efficient EC_a survey and associated soil sampling plan to reliably characterize spatial variability, an awareness and understanding of the primary factors (see Fig. 5) influencing within-field EC_a variations are crucial. Suggestions for EC_a surveys and sampling strategies are provided to account for the occurrence of the deterministic and stochastic mechanisms that create local and within-field EC_a variations.

EC_a Variation with Soil Temperature

Studies monitoring soil salinity have a temporal component, which causes concern with respect to soil temperature effects. Ideally, EC_a measurements should be referenced to 25°C using Eq. [2].

$$EC_{25^\circ C} = f_t EC_t \qquad [2]$$

where $EC_{25^\circ C}$ is the EC at 25°C (dS m^{-1}), f_t = 0.4470 + 1.4034exp($-t$/26.815) from Sheets and Hendrickx (1995) referred to as the temperature correction factor, and EC_t is the electrical conductance (dS m^{-1}) at temperature t (°C). With respect to temperature, a 1°C increase in temperature throughout the entire soil profile typically causes a 1.9% increase in the EMI EC_a signal readings. Since soil temperature fluctuations below 0.3 m in the soil profile occur rather slowly, the EC_a survey process can usually be completed before a significant change in the bulk average soil profile temperature occurs. Even though soil temperature is a routine and easy measurement, it is a measurement that can be disregarded if comparisons in a temporal study are made between data taken during the same time of day over a narrow time period (e.g., a month) when soil temperatures are relatively stable or comparisons are made for the same day of the year for long-term studies that extend for years. The idea is to compare or use EC_a data that are at the same soil temperature. If EC_a measurements are taken at or near the same soil profile temperatures, then minimal soil temperature data are needed. The soil salinity monitoring studies by Lesch et al. (1998) and Corwin et al. (2006) are examples of how to handle EC_a–directed sampling with a temporal component. If EC_a surveys must be conducted under different soil temperatures, then measuring the soil temperature profile and referencing EC_a to 25°C is necessary.

EC_a Variation with Salinity

In semiarid and arid agricultural areas, salinity is generally the soil property that dominates the EC_a measurement. Salinity accumulation occurs where evaporation or evapotranspiration exceed irrigation and/or precipitation. The predominant mechanism causing the accumulation of salt in irrigated agricultural soils is loss of water through evapotranspiration, leaving ever increasing concentrations of salts in the remaining water. Apparent soil electrical conductivity is not generally used as a direct measure of soil salinity, particularly at EC_a < 1 dS m^{-1}, where the influence of conductive soil properties other than salinity can have an increased influence on the EC_a reading. As a general rule, at EC_a values greater than about 1 dS m^{-1} salinity is usually dominating the EC_a reading; consequently, geospatial EC_a measurements are most likely mapping soil salinity.

Unlike texture and bulk density, which are static properties of soils, salinity is a comparatively dynamic property. It varies temporally and spatially with depth and across the landscape and exhibits high variation across a field and moderate to high local-scale variability (Corwin et al., 2003b). Local-scale variation determined from near-surface furrow samples acquired 0.5 m apart can vary anywhere from 10 to 100% due to micro-scale soil composition characteristics and/or fluctuations in preferential water flow.

Electromagnetic induction instrument readings tend to average out this local-scale variation. The degree to which this averaging occurs depends directly on the instrument's "footprint" (i.e., the volume of soil incorporated into the signal response). For example, an EM-38 signal will be influenced by any electrically conductive material within about 1 to 2 m of the instrument (both laterally and vertically). Hence, it is typically assumed to have a footprint of about 2 m^3. Because the volume of soil measured by the EM-38 is so much larger than the volume obtained by conventional soil sampling techniques, an estimate of the degree of local-scale salinity variation needs to be acquired for calibration model purposes and for soil quality assessments of spatial variability. Such an estimate can be acquired by obtaining duplicate or replicate sample cores within a 1-m radius at some of the calibration sites during the soil sampling process. The replicate cores can then be used to estimate the local-scale salinity variation (referred to as the "nugget variation" in geostatistical models and as the "pure error estimate" in spatial regression models). The measured salinity data from these cores can be used to construct a residual autocorrelation test, known as a "lack-of-fit" test, for assessing the spatial residual independence assumption (Lesch et al., 1995a). Techniques for estimating the local-scale salinity variation and performing residual lack-of-fit tests were described in Lesch et al. (1995a).

In a typical 12 to 16 site calibration sampling design, replicate sample cores are commonly taken at three to four of the calibration sites. These three to four sites can either be chosen at random (from among the 16 sites) or selected throughout the survey area. Additionally, the core separation spacing should be the same at all sites, and both the primary and replicate cores should always come from the same location with respect to the bed–furrow (or drip line) environment (i.e., both from the bed, or both from the furrow).

Variations in salinity through the soil profile also influence the EC_a measurement. This influence is particularly complex when EC_a is measured with EMI because the depth-weighted response function of the instrument (e.g., EM-31 or EM-38) is nonlinear. The depth-weighted nonlinearity is reflected in Eq. [3–4], which illustrate the cumulative relative contributions to EC_a [i.e., $R(z)$] for a homogeneously conductive material below a normalized depth of z based on for vertical and horizontal dipoles, respectively:

$$R_v(z) = \frac{1}{(4z^2+1)^{1/2}} \qquad [3]$$

$$R_h(z) = (4z^2+1)^{1/2} - 2z \qquad [4]$$

When considering 0.3-m depth increments through the soil profile, the greatest response for EM_h occurs over the 0- to 0.3-m depth increment and over the 0.3- to 0.6-m depth increment for EM_v. Nevertheless, it is possible to determine the general shape of the salinity profile by the relative magnitudes of the EM_h and EM_v readings at a point in the field. For salinity-driven EC_a surveys, if $EM_h > EM_v$, then the salinity profile is inverted and decreases with depth. If $EM_h < EM_v$, then salinity increases with depth. If salinity is uniform, then $EM_h \approx EM_v$.

EC_a Variation with Water Content

Soil water content variations affect EC_a measurements (Rhoades et al., 1976). Like salinity, soil water content is a dynamic soil property that varies with depth and across the landscape, generally with moderate to high local-scale variability. In areas under uniform irrigation management practices or natural rainfall, the degree of spatial water content variability is typically minimal provided significant soil texture variation is not present. However, some fields demonstrate gradual trends in water content across the extent of the field, which may be due to gradual changes in shallow water table levels close to the depth of penetration of measurement, textural gradations, or nonuniformity of water application (e.g., flood irrigation establishes a trend of high to low soil water content from the head water to tail water ends of a field, respectively). In instances where gradual trends occur in the soil water content level, trend surface parameters in the regression model can be used.

Like salinity, variations in the water content through the soil profile influence the EC_a measurement, and this influence is particularly complex when using EMI. As with salinity, it is possible to determine the general profile shape of water content. For fields where water content is the dominant soil property influencing the EC_a measurement, if water content decreases with depth, then $EM_h > EM_v$. If water content increases, then $EM_h < EM_v$. If water content is uniform, then $EM_h \approx EM_v$.

It is important to remember that if the water content of the soil drops too low (e.g., <50–70% of field capacity), then the EMI signal readings can become unreliable. In most practical applications, reliable EMI signal data will be obtained when the soil is at or near field capacity. Surveying dry areas should be avoided. This is especially true for surveys that use ER, which requires close contact between the electrodes and soil that can only be attained when the soil surface is moist.

The original general protocols by Corwin and Lesch (2005b) indicated that field-scale EC_a surveys should be conducted at or near field capacity across the entire field, but did not specify the range of water contents. Field capacity refers to the water content at approximately 1/3 bar, and in the field is taken to represent the water content at which free drainage no longer occurs, which generally occurs 2 to 4 d following a rainfall or irrigation (Peters, 1965). In a subsequent paper by Corwin and Lesch (2013), data were presented showing that between 50 and 70% of field capacity the conductance pathways in the solution phase are broken, causing spurious EC_a measurements. Corwin and Lesch (2013) found that at least 70% of field capacity is needed down to the depth of penetration of the geophysical EC_a approach (e.g., ER or EMI) to prevent spurious results from occurring caused by discontinuous conductance pathways in the soil solution phase. As a general rule, georeferenced EC_a data collection should be conducted only when the water content through the soil profile of interest is above 70% of field capacity and preferably as close to field capacity as possible. A gray area exists in the range of 50–70% of field capacity. Surveys of EC_a are substantially affected below 50% of field capacity and should not be conducted on soils that are this dry.

Sufficient water content is needed down to the depth of penetration of the geophysical approach to prevent spurious and misleading measurements. This has significant ramifications, particularly for EC_a surveys conducted on dryland farms, since EC_a surveys should only be conducted after sufficient rainfall has occurred (or sufficient irrigation water has been applied on irrigated crop land) to wet up the soil profile to the appropriate depth of penetration of the EC_a measurement instrumentation. If this precaution is not taken, the reliability of the EC_a survey is dubious. Failure to conduct an EC_a survey within the identified range of water contents can result in spurious data that will render false conclusions about the target property or properties.

EC_a Variation Induced by Changes in Soil Texture

Soil texture can cause extremely complex spatial patterns of EC_a. Under a uniform irrigation distribution, water content will generally coincide with texture—soils higher in sand have lower water contents than soils higher in clay. Minimal complexities in spatial patterns of EC_a occur (i) when there is minimal soil texture variability, (ii) when the texture changes are smooth and gradual across the field, or (iii) when the texture, water content, and salinity variations are strongly correlated.

In instances where soil texture is highly spatially variable, the ability to characterize that variability may be difficult with only geospatial measurements of EC_a. Heil and Schmidhalter (2012) utilized linear multivariate regression analysis to calibrate soil texture to EC_a and other parameters:

$$Y = \beta_0 + \beta_1 x_1 + \beta_2 x_2 + \cdots + \beta_n x_n + \varepsilon \qquad [5]$$

where the response variable (Y) represents the target soil property (i.e., texture as measured by sand, silt, and clay percentage); $\beta_0, \beta_1, \beta_2, \ldots, \beta_n$ represent the empirical regression model coefficients; $x_1, x_2, \ldots, x_n$ represent terrain attributes, EC_a, cultivation, and fertilizing parameters, as well as the boundary of Quaternary sediments; and ε represents the residual error component associated with the model. Multivariate models relating EC_a and other edaphic properties to a target property are common, particularly when the target property is highly spatially variable.

EC_a Variation Induced by Other Edaphic Properties

These properties include bulk density, OM, magnetic susceptibility, and presence of resistive material (e.g., gravel, rocks, clay layers, bedrock). Generally, significant variation in these properties needs to be present before a meaningful influence on the EC_a signal reading occurs. In general, bulk density does not vary to a significant degree across a field of 10 to 30 ha. Sharp variation in bulk density is usually associated with anthropogenic influences, such as compaction due to farm vehicles, as discussed in Step 2. Magnetic susceptibility is seldom a factor except for soils high in free iron oxides. In contrast, OM can vary spatially, but generally from one soil type to another and rarely in arid and semiarid soils does OM have any significant influence on EC_a because OM tends to be <2% and tends to be oxidized quickly. Organic matter is more of a concern in the Midwest and southeastern United States and other areas of the world with similar propensities to accumulate OM due to climate. In these areas, slope and aspect will influence the accumulation of OM, particularly in gullies and depressions. Apparent soil electrical conductivity variation related to OM was investigated by Jaynes (1996). Walter et al. (2015) mapped peatlands using EC_a.

Variation in EC_a can be the consequence of variations in the depth to clay layers (Doolittle et al., 1994), water table (Schumann and Zaman, 2003), and impermeable layers such as bedrock or $CaCO_3$ layer (Jansen et al., 1993; Doolittle et al., 2002). In cases where these resistive or conductive layers are within 1.5 m of the soil surface, a significant effect on the reading will likely occur. For this reason, EC_a surveys should not be conducted in areas where the depth to these layers is less than the depth of penetration of the EC_a measurement equipment unless the objective of the survey is to locate these layers. If depth to clay layers, water table, or impermeable layers is not the target property, then some means of avoiding their influence is necessary, such as keeping the depth of measurement of EC_a above these layers. As an example, this is achieved by taking only EM_h measurements of EC_a or by narrowing the interelectrode spacing of ER to be less than the depth to the water table or impermeable layer.

EC_a Variation with Depth

The variation of EC_a with depth is primarily due to gradations in salinity, texture, and water content through the soil profile. Soil salinity levels can change quite rapidly with depth; it is not unusual in some arid zone areas to see relative salinity profile levels fluctuate by an order of magnitude within the top meter of soil. Salinity will vary in the soil profile primarily from the process of leaching, with plant, chemical, and topographic effects contributing to variations. Water content tends to increase with depth and will vary according to textural distribution. Textural distribution is mainly a consequence of soil formation processes. However, anthropogenic effects can result in increased uniformity of texture within the plow layer or can produce other localized variations.

Devising a sampling scheme that accounts for temporal and depth variations while maintaining accurate and consistent sampling depths throughout a survey area is critical. Without prior knowledge of the distribution of salinity, water content, and texture within a profile, it can be difficult to infer the appropriate sample depth design. For this reason, soil cores should be acquired to a depth of at least 1.2 to 1.5 m at each sample site. If laboratory analysis resources permit, each core can be sliced into depth increments, thereby facilitating the estimation of prediction functions (e.g., regression models) for multiple sample depths.

Electrical resistivity and EMI techniques are both well suited for field-scale applications because their volumes of measurement are large, which reduces the influence of local-scale variability. Electrical resistivity has a flexibility that has proven advantageous for field application; that is, the depth and volume of measurement can be easily changed by altering the spacing between the electrodes. This allows the EC_a for a discrete depth interval of soil to be easily calculated with a fixed-array four electrode by measuring the EC_a of successive layers for increasing interelectrode spacing and using the following equation (Barnes, 1952; Telford et al., 1976):

$$EC_{a,x} = EC_{a,x_i} - EC_{a,x_{i-1}} = \left(\frac{EC_{a,x_i} x_i - EC_{a,x_{i-1}} x_{i-1}}{x_i - x_{i-1}} \right) \quad [6]$$

where x_i is the interelectrode spacing, which equals the depth of sampling, x_{i-1} the previous interelectrode spacing, which equals the depth of previous sampling, and $EC_{a'x}$ the apparent soil electrical conductivity for a specific depth interval. However, this approach is an estimation of the conductance profile and has been improved on by combining inverse modeling with electrical resistivity tomography (ERT) or with EMI instrumentation having dual-geometry receivers at multiple separations from the transmitter (e.g., DUALEM-421).

Aside from using EMI instrumentation such as the DUALEM-421 with multiple intercoil spacing, single dipole EMI instrumentation with single intercoil spacing (e.g., EM-38) can also measure EC_a at variable depths by positioning the EMI instrument at various heights above the soil surface in either the vertical (EM_v) or horizontal (EM_h) dipole mode (Rhoades and Corwin, 1981; Corwin and Rhoades, 1982). Similar to ERT, depth profiling of EC_a with EMI is mathematically complex (Borchers et al., 1997; McBratney et al., 2000; Hendrickx et al., 2002b). Though not required, the measurement of EC_a near the soil surface (i.e., top 0.25–0.5 m) along with spatially associated larger soil volume EC_a measurements with EMI equipment can be used to increase the accuracy of the fitted prediction functions that define EC_a profile variation (Lesch et al., 1992). Most recently, Triantafilis and Monteiro Santos (2010) used inverse modeling of EM-38 and EM-31 signal data to profile soil salinity. The introduction of EMI instrumentation such as the DUALEM-421 makes the collection of EC_a data for profiling salinity and other target properties easier, causing heightened interest in research in the inverse modeling of EC_a measurements.

The depth of penetration of an EMI sensor is theoretically calculated from the skin depth in Eq. [7]:

$$\text{One skin depth} = \frac{1}{\alpha} = \frac{1}{\omega \left\{ \frac{\mu\varepsilon}{2} \left[\left(1 + \frac{\sigma^2}{\varepsilon^2 \omega^2} \right)^{1/2} - 2 \right] \right\}^{1/2}} \quad [7]$$

where one skin depth is the depth (in meters) at which the signal is attenuated by $1/e$ (about 0.37), α is the attenuation constant in the wave equation (Balanis, 1989), σ is the subsurface electrical conductivity, μ is the subsurface magnetic permeability, ω is the angular frequency, and ε is the subsurface electrical permittivity. However, many of the parameters in Eq. [7] are spatially variable, so an empirical alternative has been developed to estimate the field-specific depth of penetration of any EC_a sensor. Soil samples are acquired at each sample site (location of the sample sites are established in Step 4) in 0.3-m increments, typically down to a depth of either 1.2 or 1.5 m. Correlations between EC_a and the target property at various composite depths (e.g., 0–0.3, 0–0.6, 0–0.9, 0–1.2, and 0–1.5 m) are performed. The composite depth with the highest correlation is taken as the depth of penetration of the instrument. In resistive soils the EMI signal travels deeper and in conductive soils the signal remains shallower as it dissipates more readily.

Step 4: Soil Sample Design Based on Georeferenced EC_a Data

Once a geo-referenced EC_a survey is conducted, the data are used to establish the locations of the soil core sample sites for calibration of EC_a to the target property. To establish the locations where soil cores are to be taken, either design-based (i.e., probability-based) or model-based (i.e., prediction-based) sampling schemes are used (Corwin and Lesch, 2005b). Design-based sampling schemes (e.g., simple random sampling, stratified random sampling, unsupervised classification, cluster sampling) have historically been the most commonly used and hence are more familiar to most research scientists. In general, design-based sampling relies on randomization principles for drawing statistical inference (Lesch, 2012). The underlying theory supporting the use of design-based sampling strategies is well developed and clearly explained by Thompson (1992) and Brus and DeGruijter (1993). Thompson (1992) provides an overview of multiple types of design-based sampling methods. The aim of design-based sampling methods is not to estimate models. Design-based methods can be useful whenever the reason for sampling does not involve spatial modeling; for example, when soil properties (e.g., organic matter content) over different fields are compared. Unfortunately, design-based sampling is less than ideal when the aim is to build a spatial model (e.g., maps, pedotransfer functions, plant–soil models). In this case, model-based and (in the case when no covariates are available) grid sampling are preferred.

Model-based sampling strategies are designed to support the use of parametric modeling (Lesch, 2012) by explicitly focusing on the requirements of a specific kind of modeling that one intends to use, such as avoiding residuals autocorrelation in linear regression modeling (Hengl et al., 2003; Lesch, 2005a) or minimizing kriging variance (Van Groenigen et al., 1999). The underlying theory behind this approach for finite population sampling is discussed by Valliant et al. (2000). Lesch (2005a) and Corwin et al. (2010) compare model-based and design-based sampling strategies in detail, highlighting some of the strengths of model-based sampling approaches.

The validity and effectiveness of a sampling strategy is fundamental to the EC_a–directed soil sampling approach. Recent validation and comparison studies of model- and design-based sampling strategies for characterizing the spatial variability of soil salinity with EC_a–directed soil sampling have indicated that the model-based sampling approach resulted in better model discrimination, more precise parameter estimates, and smaller prediction variances than the design-based sampling strategy (Lesch and Corwin, 2008; Corwin et al., 2010). Even though a model-based sampling design, such as a response surface sampling design, has been less prevalent in the literature, it is concluded from the comparison that there is no reason to refrain from its use and, in fact, warrants equal consideration. The clear advantage of the model-based sampling design, and more specifically the use of a response surface sampling design, is that there is a substantial reduction in the number of samples required to characterize the variation in the soil property of interest as compared to other approaches. A drawback is that the level of technical knowledge in the use of software such as ESAP (Lesch et al., 2000), which uses the response surface sampling design approach, is greater than other statistical software.

Several examples of design- and model-based sensor-directed soil sampling are available in the literature. In this section an overview of a selected group of these methodologies is presented, with particular focus on model-based soil sampling for soil mapping through ordinary least square regressions with remote and proximal sensor data. The case of model-based (and grid-based) sampling when no covariate information is available is also discussed.

To map soil property data when no ancillary data are available either deterministic (e.g., spline, inverse distance weighting) or geostatistical (e.g., kriging) interpolation methods are used. When no ancillary information is available, systematic sampling, as opposed to clustered or random sampling, is expected to perform best for reliable and accurate spatial interpolation (Zimmerman et al., 1999; Roberts et al., 2004). Systematic sampling is a special case of dispersed sampling, which includes all schemes where the average distance between neighbors is significantly greater than it would be for a random distribution (Mitchell, 2005), where the distance between nearest neighbors is fairly uniform for all the sampling locations and clustering is not (or rarely) observed. Grid sampling is often employed to map soil properties with kriging because it is an effective way to minimize the average interpolation error (Burgess et al., 1981; Burgess and Webster, 1984). Gridded sampling can be laid out by dividing the area of interest in regular polygons (e.g., squares, diamonds) and then selecting the center of each polygon as a sampling location (aligned systematic grid) or selecting a random point within the polygon as a sampling location (non-aligned systematic grid).

Another efficient way of obtaining dispersed sampling schemes is through space-filling algorithms. Grid sampling does not guarantee even-space filling (i.e., maximization of the dispersion of the sampling locations), especially when study areas are irregularly shaped. In this case, model-based sampling optimization can be employed. Van Groenigen et al. (2000) proposed a solution for this issue by means of the minimization of the means of the shortest distances (MMSD) criterion. The MMSD criterion aims to minimize the expectation of the distance of an arbitrary (unsampled) point to its nearest sampling location. Van Groenigen et al. (2000) showed how to find the best fitness for the MMSD criterion with a spatial simulated annealing (SSA) approach. The SSA approach allows for a random perturbation of an initial set of locations to be replaced by a new set of sampling locations, as far as the fitness of the function describing the MMSD criterion is improved (i.e., minimized). Local minima of the fitness function are avoided by the use of the Metropolis criterion (Metropolis et al., 1953). The fitness function will, after a certain number of iterations "freeze" over a particular set of sampling locations that best satisfy the MMSD criterion. This approach can be employed using the freeware platforms SANOS (Van Groenigen et al., 2000) and MSANOS (Barca et al., 2015). As an alternative to the MMSD criterion, other space-filling criteria can be used, such as the mean squared shortest distance (MSSD) criterion, also optimized in a SSA fashion, available in the R (R Development Core Team, 2012) package spsann (Samuel-Rosa et al., 2015).

When no covariate information is available, one should sample the site of interest to sufficiently represent the spatial variation of the target soil property. Unfortunately, the number of sampling locations needed to properly model the spatial variation of the target property cannot be determined a priori as it is highly variable and site specific. Indeed, it is common to observe different spatial structure (e.g., different semivariogram structure) for different properties at the same field, or for the same property at different fields. To overcome the uncertainty about the spatial structure of the target soil property, it is advisable to use as many sampling locations as possible. A high number of sampling locations is also advisable to increase the spatial resolution (i.e., block support, pixel size) of the resulting soil map (Hengl, 2006).

Monetary and time constraints usually limit the number of soil samples taken at a study field to characterize spatial variability. The use of intensively sampled ancillary information provided by on-the-go sensors (e.g., ER and EMI) or remote sensing imagery helps to understand the spatial structure of a target soil property with high resolution and coverage, and, concurrently, reduces the number of soil samples needed to properly characterize the spatial variation of a target soil property (Viscarra Rossel et al., 2011). Soil samples are needed to establish a calibration between the target soil property and sensor data. Once the sensor data are calibrated, its data can be used to model the spatial variability of the target property.

Several sampling designs have been presented in the literature. These sampling designs include, but are not limited to: Lesch et al.'s (2000) response survey sampling design (Lesch, 2005a; Fitzgerald et al., 2006; Corwin et al., 2010; Guo et al., 2015), Van Groenigen et al.'s (2000) minimization of a weighted means of the shortest distance (Barca et al., 2015; Brus and Heuvelink, 2007; Castrignanò et al., 2008; Debba et al., 2005; Scudiero et al., 2011), Minasny et al.'s (2007) variance Quad-Tree algorithm (Li et al., 2007; Yao et al., 2012), balanced sampling (Brus, 2015), and a special case of the latter known as Minasny and McBratney's (2006) conditioned Latin hypercube (Clifford et al., 2014; Kidd et al., 2015; Ließ, 2015).

Many spatial modeling techniques can be used with ancillary data, including regression kriging, co-kriging, and linear regression. Often, soil mapping accuracy relies much more on gathering more useful and higher quality data than using sophisticated statistical methods (Minasny and McBratney, 2007). One of the ways to improve the quality of field data is the selection of an appropriate sampling strategy for the selected modeling technique (Lesch et al., 1995a). Indeed, different sampling strategies support certain types of modeling better than others. Consider the following examples. With interpolation methods such as regression kriging, a sufficient number of soil sampling locations should be selected to support the spatial interpolation of the model residuals. When using regression modeling, attention is given to maximize the distance between soil samples to assure spatial independence of the regression errors (Hengl et al., 2003; Lesch, 2005a). When the covariate data show nonstationarity, a variance Quad Tree approach to soil sampling optimization is suggested to improve geostatistical modeling (Minasny et al., 2007).

In EC_a–directed soil sampling, a calibration between the target soil property and EC_a sensor data with ordinary regression is established followed by interpolation of the intensively surveyed ancillary information using techniques such as ordinary kriging or inverse distance weighting. Regression modeling is chosen because of its relative simplicity, requirement of fewer soil samples, and similar performance to more sophisticated modeling techniques.

Ordinary least square (OLS) regression modeling represents a special case of a much more general class of models commonly known as linear regression models with spatially correlated errors (Schabenberger and Gotway, 2004), hierarchical spatial models (Banerjee et al., 2014), or geostatistical mixed linear models (Haskard et al., 2007).The latter class of models includes many of the geostatistical techniques familiar to soil scientists, including universal kriging and kriging with external drift, as well as OLS regression and analysis of covariance models (Lesch and Corwin, 2008). At a selected field, a suitable linear equation can be specified that relates the target soil property of interest to a linear combination of sensor measurements and (possibly) trend surface coordinates. Refer to Lesch and Corwin (2008) and Lesch (2012) for in-depth description of the use of OLS regression for prediction of spatial soil property information from ancillary sensor data. These suggested publications include extensive details on model derivations, residual assumptions, and model validation tests.

An example of a linear EC_a soil sensor calibration equation is:

$$y_i = f\left(x_{1,i}, x_{2,i}, \ldots, x_{n,i}, c_{x,i}, c_{y,i}\right) + \varepsilon_i \qquad [8]$$

where y is the dependent variable (i.e., the target soil property, e.g., EC_e) at each ith location, x is the sensor readings for n EC_a soil sensor measurements, and c_x and c_y are the associated ith survey site coordinate locations. A random error component, ε, is associated with the model at each ith location. Equation [8] can be viewed as a "signal (i.e., sensor readings) + trend (i.e., coordinates)" model (Lesch, 2012). The trend surface components are optional and should only be included if they are found to be necessary (i.e., if the associated regression parameter estimates are statistically significant or if the inclusion of such components is needed to address an obvious spatial trend in a residual plot). Multiple OLS regression analysis makes several key assumptions, including: no or little multicollinearity between explanatory variables, homoscedasticity, and normality of the residuals (Achen, 1982). The optimal estimation of Eq. [8] or similar regression models depends on the assumptions placed on the spatial randomness of the error component. If the errors can be assumed to be approximately uncorrelated, then OLS fitting techniques can be used (Lesch and Corwin, 2008). The Moran's I test for residual spatial autocorrelation (Cliff and Ord, 1981) can be used to test for this assumption. Lesch and Corwin (2008) and (Mitchell, 2005) provide a detailed description on the definition and calculation of this test. Commercial software platforms, such as SAS (SAS Institute Inc.) and ArcMap (ESRI) feature tools for the calculation of Moran's I test. Alternatively, the spdep library (Bivand et al., 2011) in R can also be used. If the errors are observed to be autocorrelated, then the model can be efficiently estimated using maximum likelihood or restricted maximum likelihood fitting techniques, which account for the spatial structure of the residuals (Littell et al., 2006). Such model estimation is supported by several commercial software platforms (e.g., SAS), but is also available in the spdep library in R. As an alternative to the maximum likelihood approach, regression kriging can be used if there are enough samples to support the spatial interpolation of the regression errors.

The likelihood of the residual errors being approximately uncorrelated depends primarily on (i) the method used to select the calibration sampling sites and (ii) the degree to which the explanatory variables correlate with the response variable of interest. The stronger the correlation between sensors and target soil variable, the more likely the regression errors will be spatially uncorrelated (Lesch, 2005a; Lesch and Corwin, 2008). The strength of the calibration cannot be known a priori. However, sampling schemes can be optimized to minimize the chance of observing spatial autocorrelation between residuals, by maximizing the distance between soil samples. Two model-based sampling strategies that can be used to optimize soil sampling schemes to support OLS modeling are Lesch et al.'s (2000) response surface sampling design (RSSD) and Van Groenigen et al.'s (2000) minimization of the weighted means of shortest distance (MWMSD). The aims of both strategies are (i) to ensure that the covariates' spatial structures are properly represented within the limited number of locations where the soil is to be sampled and (ii) to obtain a dispersed sampling scheme to minimize the chance of observing spatial autocorrelation between residuals.

Response Surface Sampling Design

The RSSD is tailored to optimize the calibration of intensively surveyed soil sensor data to soil analysis of a target property or properties using OLS linear regression modeling (Lesch et al., 2000). The RSSD aims to select a limited number of soil samples (m) to (i) optimize the estimation of the regression parameters and (ii) to eliminate or minimize the effects of the spatially dependent error structure on the estimation process. The RSSD optimization is a multistep procedure:

Step 1. The sensor data are transformed into a centered, scaled, and decorrelated matrix via principal components analysis (PCA).

Step 2. A traditional response surface approach (Myers et al., 2009) is selected to, theoretically, facilitate the optimal parameterization of the model associated with the PCA matrix.

Step 3. An initial set of q "candidate" locations is selected ($q > m$) from the PCA matrix that best match the m design levels specified by the response surface design from Step 2.

Step 4. An interactive algorithm, aiming to maximize some function of the minimum separation (Euclidean) distance between adjacent site locations, is used to select a set of m sampling locations from the q candidate sites.

Step 4 is necessary to minimize (or eliminate) possible short-range residual correlation effects and to support the use of OLS modeling. Further details about the principles of the RSSD methodology can be found in Lesch et al. (2000) and Lesch (2005a). The RSSD has been tested on a variety of sensors, including EC_a (Lesch, 2005a), remote sensing imagery–surface reflectance (Fitzgerald et al., 2006), and radar data (Guo et al., 2015). The RSSD has been previously validated against classical, non-model-based designs, such as stratified random sampling (Corwin et al., 2010) and grid sampling (Guo et al., 2015), showing optimal performances for the calibration of soil sensor data with soil properties.

The freeware ESAP (Lesch et al., 2000) can be used to optimize the RSSD sampling scheme. The ESAP software is stand-alone freeware that works in the Windows (Microsoft, version XP or higher) environment. Response surface sampling design optimization with ESAP is generally characterized by short computing times (minutes), which is beneficial, especially when working with on-the-go sensors. As explained above in this chapter, to obtain optimal sensor calibrations, soil should be sampled as soon as possible after the sensor survey, so there is little to no change in transient soil properties (e.g., water content) between sensor survey and soil sampling. ESAP can be used to select up to 20 sampling locations in a single run. Even for fairly large fields characterized by contrasting variations in soil properties, 20 RSSD samples should be sufficient for a successful calibration of the sensor measurements. If two or more sensors showing little to no collinearity were to be used, then up to 20 RSSD samples can be selected per each sensor. However, if the user feels that other soil properties of interest will not be properly represented by the available sensor data, then more sampling locations should be selected so that accurate spatial interpolations (e.g., inverse distance weighting, ordinary kriging) can be used to map the soil property or properties without using the covariate information. In such a case, ESAP can be used to select survey points in addition to the optimal initially selected locations. Because RSSD includes a space-filling algorithm, it is important to remember that buffer zones (at the field margins, along draining trenches) should be employed when using ESAP-RSSD; otherwise, such areas would be favored by the RSSD, as reported by Johnson et al. (2005) and Guo et al. (2015). As previously discussed in this chapter, the relationships between soil sensor measurements and soil properties are expected to be remarkably different at the field edges than in the rest of the field because soil properties are, generally, different at the field edges due to a variety of anthropogenic, edaphic, and meteorological factors (Sparkes et al., 1998; Corwin and Lesch, 2013).

The ESAP statistical software package estimates field-scale spatial soil property patterns from EMI signal data. It can be used to map any target soil property either directly measured by EC_a (i.e., EC_e, texture as measured by SP, water content, ρ_b, OM, CEC) or correlated with geospatial EC_a measurements at a site. ESAP consists of five modules. The ESAP-RSSD module provides an optimal soil sample design based on geospatial EC_a survey data using a response surface sampling design. The ESAP-Calibrate module uses regression or deterministic equations to predict spatial values of a target property from EC_a survey data. The ESAP-SaltMapper module maps the target soil property or properties. The ESAP-SigDPA module is preprocessing software for managing raw conductivity/GPS data files. The ESAP-DPPC Calculator module converts EC_a data into estimates of EC_e using the dual pathway parallel conductance (DPPC) model from Rhoades et al. (1989). The ESAP-DPPC module is useful in determining the quality and reliability of the EC_a and target soil property data, which is discussed later in this chapter in the section concerning data reliability tests. The ESAP freeware is available online (http://www.ars.usda.gov/Services/docs.htm?docid=15992, accessed 14 Sept. 2016).

Minimization of the Weighted Means of the Shortest Distance with Simulated Spatial Annealing

The MWMSD criterion (Van Groenigen et al., 2000) is the weighted version of the previously discussed MMSD criterion. The MWMSD criterion accounts for field shape and uneven distribution of soil properties when selecting the soil sampling locations (Scudiero et al., 2011). The MWMSD criterion aims to allocate sampling points in areas of expected maximum variations (Barca et al., 2015), but, at the same time, spreading points as far apart as possible (i.e., minimizing the Euclidean distance of any arbitrary unsampled location to the nearest sampled location).

Spatial variation of sensor measurements has been used as a weight for the MWMSD criterion. For example, Castrignanò et al. (2008), Scudiero et al. (2011), and Barca et al. (2015) used the gradient map of EC_a as a covariate. The gradient map measures the maximum differences (in degrees) between a target cell and its contiguous neighbors (i.e., high degree of change between neighboring cells indicates high local spatial variability). The freeware platform SANOS (Van Groenigen et al., 2000) can be used to optimize a sampling scheme using the MWMSD criterion. Unfortunately, support for SANOS has been discontinued. However, newer freeware featuring soil sampling selection with the MWMSD criterion through spatial simulated annealing has recently been presented (Barca et al., 2015).

The optimization of MWMSD sampling schemes generally requires long processing times (e.g., hours), which makes it improbable that soil can be sampled on the same day as when EC_a sensor measurements are acquired. Similar to RSSD, MWMSD-criterion shows a tendency to place soil samples at the field margins (Barca et al., 2015; Scudiero et al., 2011). Therefore, buffer areas along the field margins should be used to mask the sensor data to prevent the selection of soil sampling locations at field margins. In contrast to ESAP-RSSD, SANOS can be used to select more than 20 locations per available ancillary dataset.

Step 5: Soil Core Sampling at Specified Sites Designated by the Sample Design

General soil core sampling protocols (Peterson and Calvin, 1996) and associated quality control and quality assurance procedures (Klestra and Bartz, 1996) should be followed. Soil cores should be acquired to the same depth and over the same depth increments at all the selected sample sites. The depth of sampling should correspond to the depth of measurement by the ER or EMI instrumentation used to take EC_a data. Customarily soil cores are taken at 0.3-m depth increments to a depth of 1.2 or 1.5 m, which is roughly the depth of measurement of the EM-38. Soil cores should be taken directly over the location of the EC_a measurement. As the cores are taken, soil temperature through the profile can be measured at selected sites, if needed. During sampling, attention should be taken to avoid including any dry, loose soil that may have collapsed into the core hole from the soil surface.

An appropriate identification system for labeling the soil samples should be established. Any metadata associated with each sample site and the samples, such as observations about the depth to water table, abrupt changes in soil texture, horizonation, mottling, color change, and surface crusting, should be recorded. All soil samples should be placed in sealed, airtight containers to minimize the loss of moisture, which would affect water content measurements. The soil samples should be immediately placed in an insulated storage container (refrigerated, if possible) for protection and to keep the samples cool.

A crucial aspect of Step 5 that has been largely overlooked in most past EC_a–directed soil sampling studies listed in the literature review by Corwin and Lesch (2005a, 2013) is that of establishing the local-scale variation through duplicate or replicate samples at 20 to 25% or more of the sample sites. The primary and duplicate soil core samples are taken within a 0.5- to 1.0-m radius. Knowledge of the local-scale variation in comparison to global-scale variation is important because this helps to define sampling requirements (i.e., number of replicates) and to provide a perspective to the small- and large-scale variation in the target property that occurs within a field. If the local-scale variation approaches global-scale variation, then there is just as much variation within a small area (e.g., 1 m^2) as over the entire field, which makes the EC_a–directed sampling approach untenable.

Step 6: Laboratory Analysis of Soil Physical and Chemical Properties

General quality control and quality assurance protocols for laboratory analysis should be followed (Klestra and Bartz, 1996). Soil samples should be analyzed as soon as possible after their collection. All soil sample preparation and analyses should be conducted following scientifically accepted procedures such as those outlined in the Soil Science Society of America's Methods of Soil Analysis (Sparks, 1996; Dane and Topp, 2002) and the United States Department of Agriculture's Handbook 60 (US Salinity Laboratory Staff, 1954).

The appropriate analyses will depend on the objective of the study. There is general agreement by soil scientists on recommended minimum data sets of soil parameters that should be used to quantify soil quality, including biological (microbial biomass, potentially mineralizable N, and soil respiration), chemical (pH, EC_e, OM, N, P, and K), and physical (texture, bulk density, depth of rooting, infiltration, and water holding capacity) parameters (Bouma, 1989; Larson and Pierce, 1991, 1994; Arshad and Coen, 1992; Doran and Parkin, 1994, 1996). However, soil quality is a function of the intended use of the soil; consequently, the appropriate soil properties to assess quality will vary accordingly. As an example, Corwin et al. (2003b) found the following properties were appropriate for assessing quality of a salt-affected, sodic soil used for agricultural production: EC_e; pH; anions (HCO_3^-, Cl^-, NO_3^-, SO_4^{2-}) and cations (Na^+, K^+, Ca^{2+}, and Mg^{2+}) in the saturation extract; trace elements (B, Se, As, Mo) in the saturation extract; lime ($CaCO_3$); gypsum ($CaSO_4$); CEC; exchangeable Na^+, K^+, Ca^{2+}, and Mg^{2+}; exchangeable Na percentage; Na adsorption ratio; saturated hydraulic conductivity; and leaching fraction. Site-specific crop management applications generally require knowledge of those soil physical and chemical properties influencing the yield of a specific crop and impacting the environment. For instance, for an irrigated, arid zone soil located on the west side of California's San Joaquin Valley, Corwin et al. (2003a) found pH, B, NO_3^-, N, Cl^-, EC_e, leaching fraction, gravimetric water content, ρ_b, clay percentage, and SP to be the most significant soil properties when considering edaphic influences on within-field variations in cotton production.

Step 7: Stochastic and/or Deterministic Calibration of EC_a to EC_e (or Other Target Properties)

Apparent soil electrical conductivity can be calibrated to any soil property that significantly influences the EC_a measurement such as salinity (i.e., EC_e), water content, clay content, texture as measured by SP, bulk density (ρ_b), and OM. As previously mentioned, there are numerous studies that document the relationships between soil electrical conductivity and various soil physical and chemical properties, including soil salinity (Rhoades, 1992, 1996; Rhoades et al., 1989; Lesch et al., 1995a; Williams and Baker, 1982), clay content (Williams and Hoey, 1987), depth to clay layers (Doolittle et al., 1994), nutrient status (Sudduth et al., 1995), and moisture content (Kachanoski et al., 1988), to list a few. Additionally, there are articles documenting the use of conductivity survey information to determine salt loading and field irrigation efficiency (Rhoades et al., 1997; Corwin et al., 1999) and for estimating deep drainage (Triantafilis et al., 2003). All the data analysis and interpretation presented in these papers can be classified into two data modeling categories: stochastic and deterministic.

Soil salinity (i.e., EC_e) or other target properties (i.e., water content, SP, ρ_b) can be determined from EC_a in two ways: a deterministic and a stochastic approach (Rhoades et al., 1999a). The preferred approach will vary with the size of the area to be assessed, availability of equipment, and the specific objectives. The deterministic approach is the preferred approach when significant localized variations in soil type exist in the field. However, this approach typically requires knowledge of additional soil properties (e.g., soil water content, SP, ρ_b, temperature). In instances where extensive soil property information is lacking, the stochastic approach is more appropriate. In the stochastic approach, statistical modeling techniques, such as spatial regression or co-kriging, are used to directly predict the soil salinity from EC_a survey data. In this approach, the models are "dynamic" (i.e., the model parameters are estimated using soil sample data collected during the survey). The calibration is developed by acquiring soil salinity data (or other soil property data, such as SP, texture, ρ_b) from a small percentage of the EC_a measurement sites and estimating an appropriate stochastic-prediction model for each depth increment using the paired soil sample and EC_a data. Using the remaining EC_a data in conjunction with the established model, the soil salinity levels (or other calibrated properties) are predicted at all of the remaining nonsampled, measurement locations. The stochastic- and deterministic calibration approaches were described in detail by Lesch et al. (1995a, b, 2000) and incorporated into the ESAP software (Lesch et al., 2000).

In general, stochastic models are based on some form of objective sampling methodology used in conjunction with various statistical calibration techniques. Different soil sampling strategies support different types of calibration models (e.g., co-kriging, regression kriging, linear modeling). This chapter focuses on the use of linear regression methods to map soil properties in the presence of ancillary data from EMI or ER sensors. Salinity (i.e., EC_e) will be used as the target property, but any property applies that is directly measured by EC_a or correlated with geospatial EC_a measurements at a site.

According to Archie's Law (Archie, 1942) and Rhoades et al. (1976), EC_a measurements are a multiplicative function of salinity, soil tortuosity (depending on soil texture, density and particle geometry, particle pore distribution, and organic matter content), and water content. Therefore, when calibrating the EC_a measurements over a soil property (e.g., EC_e), the following power model can be used (Corwin and Lesch, 2014):

$$EC_e = \beta EC_a^{\alpha} \varepsilon^* \qquad [9]$$

where α and β are coefficients that take into account the effects of non-target edaphic factors on EC_a, and ε^* is a random (multiplicative) error component (dS m^{-1}). In Eq. [9], the error component is a multiplicative factor defined as the ratio between EC_e and the explanatory term of the equation (Tian et al., 2013). Equation [9] can be parameterized using the OLS approach, once a natural logarithm (ln) transformation is performed, so that the multiplicative nature of the EC_a–EC_e relationship becomes additive:

$$\ln\left(EC_e\right) = \ln\left(\beta\right) + \alpha \ln\left(EC_a\right) + \varepsilon \qquad [10]$$

where ε is a random (additive) error component, equal to ln(ε^*).

It is important to establish the general form of the calibration equation relating EC_a to the target property, which for demonstration purposes has been selected to be salinity or EC_e. Most calibration equations of soil properties are spatially referenced regression models. A spatially referenced regression model is just an ordinary regression equation that includes the soil property calibrated with EC_a and trend surface parameters (i.e., x and y coordinates). Accounting for trend surface parameters and the measurement of EC_a using EMI, Eq. [10] becomes

$$\ln\left(EC_e\right) = \beta_0 + \beta_1 \ln\left(EM_v\right) + \beta_2 \ln\left(EM_h\right) + \beta_3\left(x\right) + \beta_4\left(y\right) + \varepsilon \qquad [11]$$

where EC_e is the electrical conductivity of the saturation extract (dS m^{-1}); β_0, β_1, β_2, β_3, and β_4 represent the empirical regression model coefficients; x and y are the easting and northing UTM coordinates (m), and ε is the error term. If both EM_v and EM_h are reliable and there is no multicollinearity, then Eq. [11] is unchanged. However, if the EM_v data are unreliable with respect to the target property, then the β_1 ln(EM_v) term in Eq. [11] drops out, or if the EM_h data are unreliable then the β_2 ln(EM_h) term drops out.

The EC_a data should be calibrated against target soil property data that correspond to the depth of measurement of the instrument. The depth of measurement for EM_h is roughly 0.75 m and for EM_v is roughly 1.5 m. However, the depth of measurement for both EM_h and EM_v will vary from one location to the next. Consequently, it is advisable to estimate the depth of measurement for EM_h and EM_v for each field. This can be done by correlating EM_v EC_a (and EM_h EC_a) to EC_e for each composite depth of 0 to 0.3, 0 to 0.6, 0 to 0.9, 0 to 1.2, and 0 to 1.5 m. The composite depth with the highest correlation coefficient (r) is the estimated depth of penetration. Consequently, the EC_a to EC_e calibration is determined using EC_e data for the composite depth with the highest r. This, of course, suggests that soil samples need to be collected and analyzed at 0.30-m depth increments to a depth of 1.5 m at each sample site within a field. This may or may not be within the scope project resources, in which case this may not be possible. If estimating the depth of measurement for a field is not within resources, then using soil samples collected to a depth of 1.2 or 1.5 m is generally sufficient.

The study by Corwin et al. (2010) demonstrates the process of calibration. The study was a detailed survey of EC_a that was used to map soil salinity (i.e., EC_e) in an irrigated alfalfa (*Medicago sativa* L.) field near San Jacinto, CA. Figure 10 shows EM_v EC_a measurements (16122 locations) and 20 soil sampling locations selected from those measurements using a response surface sampling design. At the site, EM_h and EM_v were collinear, showing a variance inflation factor [i.e., $1(1-R^2)^{-1}$; O'Brien, 2007] of 17.2 (18.6, when ln transformed). In this example, the EM_v readings of EC_a were used to model

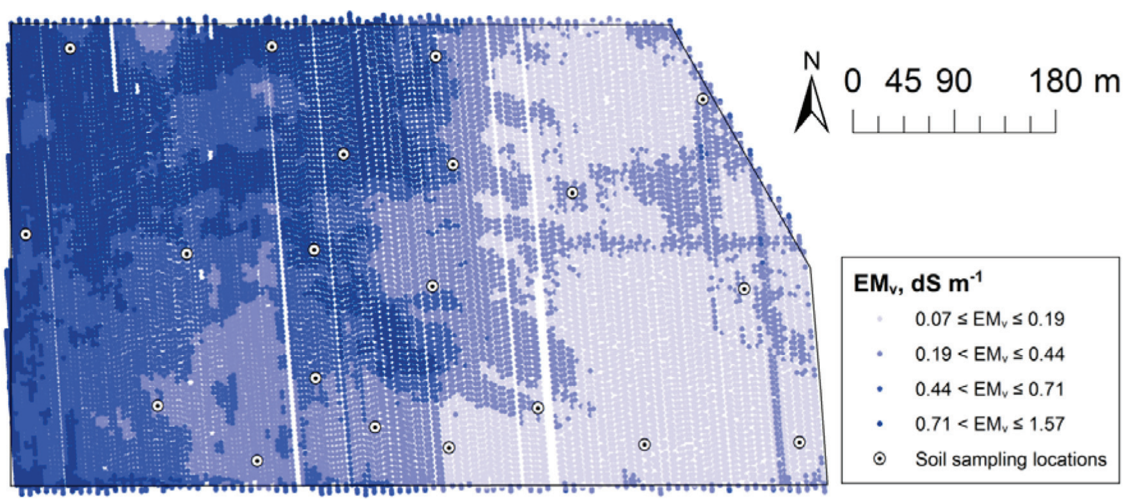

Fig. 10. Electromagnetic induction measurement in the vertical coil configuration (EM_v) of apparent electrical conductivity for the 0- to 1.5-m soil profile at 16122 survey locations across a 32.4-ha field near San Jacinto, CA.

EC_e spatial variability according to Eq. [11] with the β_2 ln(EM_h) term removed.

As an alternative to discarding the β_2 ln(EM_h) term to remove the multicollinear signal effect, one could regress the first two standardized principal component scores computed from the EM_h and EM_v readings (Lesch, 2005a). With $R^2 = 0.740$ and $F = 51.2$, the regression was significant at the $p < 0.001$ level (Fig. 11a). The intercept ($\beta_0 = 1.2 \pm 0.12$, value ± SE) and the slope ($\beta_1 = 0.65 \pm 0.09$) were both significant ($p < 0.001$). The site x and y coordinates were not included in the regression model because they were not significant. The random nature of ε was confirmed, allowing for the use of Eq. [11] in the calibration (Lesch and Corwin, 2008). The assumption of normality for ε was supported by a mean error (6×10^{-6}) that was close to zero. Residual normality was tested using the Shapiro–Wilk test (Shapiro and Wilk, 1965), which was nonsignificant. The residuals were also tested for spatial autocorrelation using the Moran's I test for spatial autocorrelation (Cliff and Ord, 1981) showing nonsignificant spatial structure. In addition to the tests on the regression assumptions, a jackknife resampling can give indications of the robustness of the model (Efron and Gong, 1983). Equation [11] was resampled (i.e., leave-one-out) and reparameterized at each iteration so that the variability in slope and intercept coefficients could be assessed in terms of jackknife variance (σ^2_{JK}):

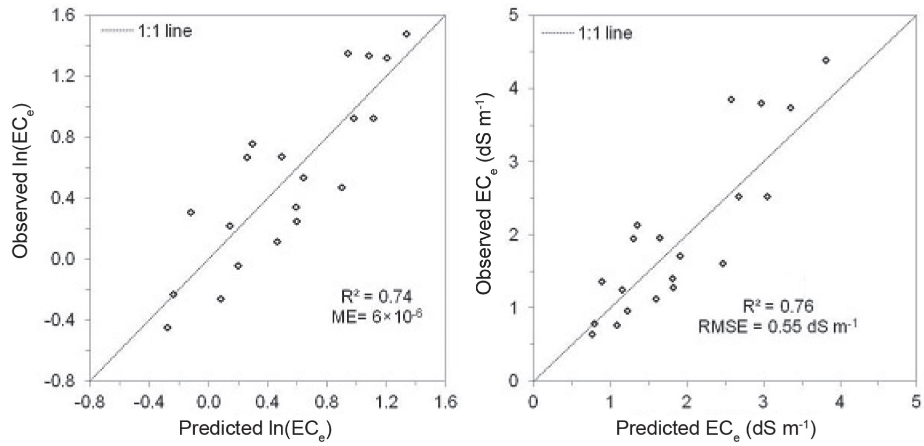

Fig. 11. Observed versus predicted (a) natural logarithm transformed soil salinity (EC_e) calculated with Eq. [10] and (b) back-transformed EC_e for a 32.4-ha field near San Jacinto, CA. Soil salinity is represented by the electrical conductivity of a saturated soil paste extract (EC_e, dS m^{-1}). R^2 is the coefficient of determination, ME is the mean error, and RMSE is the root mean square error. Dashed line is a 1:1 relationship.

$$\sigma^2_{JK} = \frac{N-1}{N}\sum_{i=1}^{N}\left(\bar{x} - \bar{x}_i\right) \qquad [12]$$

where $\bar{x}$ is the coefficient value based on all of the N (i.e., 20) samples, and $\bar{x}_i$ is the coefficient value based on leaving out the ith observation. The jackknife variances for the intercept (0.010) and slope (0.007) were remarkably small in comparison with the coefficient values based on all samples (the smaller the jackknife variance, the more robust the model). Equation [11] was back-transformed (Fig. 11b) rendering an observed–predicted $R^2 = 0.762$ and RMSE = 0.55 dS m^{-1}. Equation [11] was used to estimate EC_e at the 16122 locations (Fig. 12).

Deterministic conductivity data modeling and interpretation can be performed either from a geophysical or a soil science approach. In the geophysical approach, mathematically sophisticated inversion algorithms are generally employed. These approaches, which rely heavily on geophysical theory, have met with limited success for the interpretation of near-surface EC_a data. Part of the reason for the lack of success is that most geophysical inversion approaches assume: (i) that there are multiple conductivity signal readings available for each survey point and (ii) that distinct, physical strata differences exist within the near-surface soil horizon. Neither of these conditions are typically satisfied in most EC_a surveys.

A more common interpretation technique used, particularly in salinity inventorying work, is to employ some form of deterministic EC_a to salinity model (i.e., an equation which converts EC_a to EC_e based on knowledge of other soil properties). One model of this type that has been shown to be useful is the DPPC model developed by Rhoades et al. (1989, 1990) and extended by Lesch and Corwin (2003). This model is based on the idea that electrical conductivity of soil can be modeled as a multipathway parallel electrical conductance equation. This model has been shown to be applicable to a wide range of typical agricultural situations (Corwin and Lesch, 2003). The DPPC model demonstrates that soil electrical conductivity can be reduced to a nonlinear function of five soil properties: EC_e, SP, volumetric soil water content, ρ_b, and soil temperature. In Rhoades et al. (1990) the DPPC model was used to estimate field soil salinity levels based on EC_a survey data and measured or inferred information about the remaining soil physical properties. Corwin and Lesch (2003) and Lesch et al. (2000) showed that this model can also be used to assess the degree of influence that each of these soil properties has on the acquired EC_a–survey data.

In the deterministic approach, either theoretically or empirically determined models convert EC_a into EC_e. Deterministic models are "static" (i.e., all model parameters are considered known and no EC_e data need to be determined). For example, Eq. [13] from the DPPC model of Rhoades et al. (1989) is a deterministic approach:

$$EC_a = \left[\frac{(\theta_{ss} + \theta_{ws})^2 EC_{ws} EC_{ss}}{(\theta_{ss} EC_{ws}) + (\theta_{ws} EC_s)}\right] + (\theta_w - \theta_{ws}) EC_{wc} \qquad [13]$$

where $\theta_w = \theta_{ws} + \theta_{wc}$ = total volumetric water content (cm^3 cm^{-3}); θ_{ws} and θ_{wc} are the volumetric soil water content in the soil water pathway (cm^3 cm^{-3}) and in the continuous liquid pathway (cm^3 cm^{-3}), respectively; θ_{ss} is the volumetric water content of the surface-conductance (cm^3 cm^{-3}); EC_{ws} and EC_{wc} are the specific electrical conductivities of the soil water pathway (dS m^{-1}) and continuous liquid pathway (dS m^{-1}); and EC_{ss} is the electrical conductivity of the surface conductance (dS m^{-1}). Soil EC_a is converted into EC_e using Eq. [13–18] originally developed by Rhoades et al. (1989):

$$\theta_w = \frac{PW\rho_b}{100} \quad [14]$$

$$\theta_{ws} = 0.639\theta_w + 0.011 \quad [15]$$

$$\theta_{ss} = \frac{\rho_b}{2.65} \quad [16]$$

$$EC_{ss} = 0.019(SP) - 0.434 \quad [17]$$

$$EC_w = \left[\frac{EC_e \rho_b SP}{100\theta_w}\right] = EC_e\left[\frac{SP}{100\theta_g}\right] \quad [18]$$

where PW is the percent water on a gravimetric basis, ρ_b is the bulk density (Mg m^{-3}), SP is the saturation percentage, EC_w is the average electrical conductivity of the soil water assuming equilibrium (i.e., $EC_w = EC_{sw} = EC_{wc}$), and EC_e is the electrical conductivity of the saturation extract (dS m^{-1}).

Step 8: Spatial Statistical Analysis

In the past, the fact that EC_a is a function of several soil properties (i.e., soil salinity, texture, and water content) has sometimes been overlooked in the application of EC_a measurements to site-specific crop management. In areas of saline soils, salinity dominates the EC_a measurements and interpretations are often straightforward. However, in areas other than arid zone soils, texture and water content or even OM may be the dominant properties measured by EC_a. To use spatial measurements of EC_a in a soil quality or site-specific crop management context, it is necessary to understand what factors are most significantly influencing the EC_a measurements within the field of study. There are two commonly used approaches for determining the predominant factors influencing EC_a measurement: (i) wavelet analysis and (ii) simple statistical correlation.

An explanation of the use of wavelet analysis for determining the soil properties influencing EC_a measurements was provided by Lark et al. (2003). Even though wavelet analysis is a powerful tool for determining the dominant complex interrelated factors influencing EC_a measurement, it requires soil sample data collected on a regular grid or equal-spaced transect. Grid or equal-spaced transect sampling schemes are not as practical for determining spatial distributions of soil salinity (or some other correlated soil property) from EC_a measurements as the statistical and graphical approach first developed by Lesch et al. (1995a,b, 2000).

The most practical means of interpreting and understanding the tremendous volume of spatial data from an EC_a survey is through statistical analysis and graphic display. Details describing the statistical and graphical approach for determining the predominant soil property influencing EC_a measurements are found in Corwin and Lesch (2003). For a soil quality assessment a basic statistical analysis of all physical and chemical data by depth increment provides an understanding of the vertical profile distribution. A basic statistical analysis consists of the determination of the mean, minimum, maximum, range, standard deviation, standard error, coefficient of variation, and skewness for each depth increment (e.g., 0–0.3, 0.3–0.6, 0.6–0.9, and 0.9–1.2 m) and by composite depth (e.g., 0–1.2 m) over the depth of measurement of EC_a. In the case of EC_a measured with ER, the composite depth over the depth of measurement of EC_a is based on the spacing between the electrodes, while in the case of EM-38 measurements of EC_a the composite depth for the EM_h measurement is about 0–0.75 to 1.0 m and 0–1.2 to 1.5 m for EM_v. The calculation of the correlation coefficient between EC_a and mean value of each soil property by depth increment and composite depth over multiple sample sites determines those soil properties that correlate best with EC_a and those soil properties that are spatially represented by the EC_a–directed sampling design.

Crop yield monitoring data in conjunction with EC_a survey data can be used from a site-specific crop management perspective to (i) identify those soil properties influencing yield (Corwin et al., 2003a) and (ii) delineate site-specific management units (Corwin and Lesch, 2010). For site-specific crop management, an understanding of the influence of spatial variation in soil properties on within-field crop-yield (or crop quality) variation is desired. To accomplish this using EC_a, crop yield (or crop quality) *must* correlate with EC_a within a field. If crop yield (or crop quality) and EC_a are correlated, then basic statistical analyses by depth increment (e.g., 0–0.3, 0.3–0.6, 0.6–0.9, and 0.9–1.2 m) and by composite depths (e.g., 0–0.3, 0–0.6, 0–0.9, and 0–1.2 m) are performed. As before, the correlation between EC_a and mean values of each soil property for each depth increment and each composite depth establishes those soil properties that are spatially characterized with the EC_a–directed sampling design. The correlations between crop yield (or crop quality) and physical and chemical soil properties will also establish the depth of concern (i.e., the root zone of the crop), which will be the composite depth that consistently has the highest correlation of each soil property (i.e., each soil property determined to be significant to influencing yield) with crop yield (or crop quality). Exploratory graphical analyses (i.e., scatter plots of crop yield or crop quality and each soil property) are then conducted for the depth of concern to determine the linear or curvilinear relationship between the significant physical and chemical properties and crop yield (or crop quality). A spatial linear regression is formulated that relates the significant soil properties as the independent variables to crop yield (or crop quality) as the dependent variable. The functional form of the model is developed from the exploratory graphic analysis. The model is adjusted for spatial autocorrelation, if necessary, using restricted maximum likelihood or some other technique. This entire spatial statistical analysis process is clearly demonstrated by Corwin et al. (2003a) and Corwin and Lesch (2005c).

To use spatial measurements of EC_a in a site-specific crop management context, it is not only necessary to understand what factors most significantly influence EC_a measurements within the field of study, but also to know those factors that most significantly influence within-field variation in crop yield (or crop quality). Corwin et al. (2003a) used sensitivity analysis simulations to arrive at the dominant edaphic and anthropogenic factors influencing within-field cotton yield variations. Sensitivity analysis involves increasing a single independent variable (i.e., edaphic factors) and observing the resultant effect on the dependent variable (i.e., crop yield or crop quality). This is done for each independent variable. The relative effect of each independent variable on the dependent variable determines the independent variable that most significantly influences the dependent variable.

Step 9: GIS Database Development

The organization, manipulation, and graphic display of spatial soil and EC_a data are best accomplished with GIS. Spatial soil property data are entered into any of the several commercially available GIS software packages, such as ArcGIS. Once the spatial data are entered, maps of the soil physical and chemical properties can be easily prepared.

Step 10: Graphic Display

Step 10 focuses on the methods of interpolation that are available to display the spatial distribution of a target property or other properties. Inverse distance weighting (IDW), cubic spline, and various geostatistical approaches are the prevalent choices. Previous studies comparing interpolation methods have met with mixed results. In some instances kriging has been found to perform the best (Laslett et al., 1987; Warrick et al., 1988; Leenaers et al., 1990; Kravchenko and Bullock, 1999), and in others IDW has been found superior (Weber and Englund, 1992; Wollenhaupt et al., 1994; Gotway et al., 1996). A common means of determining which method is the best to use for a particular spatial data set is to use the statistical approach of jackknifing to establish the interpolation method that minimizes the prediction error (Isaaks and Srivastava, 1989). Bourgault et al. (1997) provided a useful toolbox of geostatistical approaches used on a soil salinity data set and advised the use of cross-validation to identify the approach that is best. The advantage of using a geostatistical approach for interpolation over IDW or cubic spline is an assessment of spatial uncertainty that can be obtained from geostatistical approaches.

As an example, the EC_e estimations in Fig. 12a were interpolated to obtain continuous salinity values across the field shown in Fig. 12b. The EC_e estimations showed a northeast–southwest trend. Therefore, the point data were interpolated using universal kriging (UK). The data were normalized with a natural logarithm transformation. To carry out the interpolation, the spatial correlation structure of soil salinity was modeled by an isotropic exponential semivariogram, $\nu[\ln(EC_e)]$:

$$\nu\left[\ln\left(EC_e\right)\right]=\left(\eta+\sigma^2\right)\left[1-\exp\left(-\frac{h}{r}\right)\right] \quad [19]$$

where η represents the nugget variance, σ the spatial variance component (partial sill), h the lag distance, and r the range. Specifically, η was 0, σ was 0.078, and r was 280 m. The interpolation was performed using a minimum of 20 and maximum of 40 neighbors using Arc Map (version 10.1, ESRI). The interpolated surface was characterized by a leave-one-out cross-validation R^2 of 0.989 and RMSE of 0.09 dS m^{-1}. A salinity map interpolated using IDW would have returned leave-one-out cross-validation R^2 of 0.985 and RMSE of 0.10 dS m^{-1}. This marginal difference in performance between geostatistical (UK) and deterministic (IDW) interpolation methods indicates that, when dealing with very intensive sensor measurement grids, less sophisticated interpolation techniques can be employed, leading to results of equivalent quality. The UK (point) interpolation was used to create a soil salinity map on a 2 × 2 m support (Fig. 12b). When compared with the 20 soil samples, the mapped salinity values showed R^2 of 0.753 and RMSE of 0.56 dS m^{-1}. The salinity prediction accuracy slightly degenerated from Eq. [10]. The build-up of error throughout the procedure should always be considered when mapping soil properties (Heuvelink, 1998). Nelson et al. (2011) described a methodology to budget error in soil mapping according to different sources of uncertainty (e.g., GPS positioning, soil sampling and laboratory malpractice, weak relationships between target soil property and sensor data, interpolation errors).

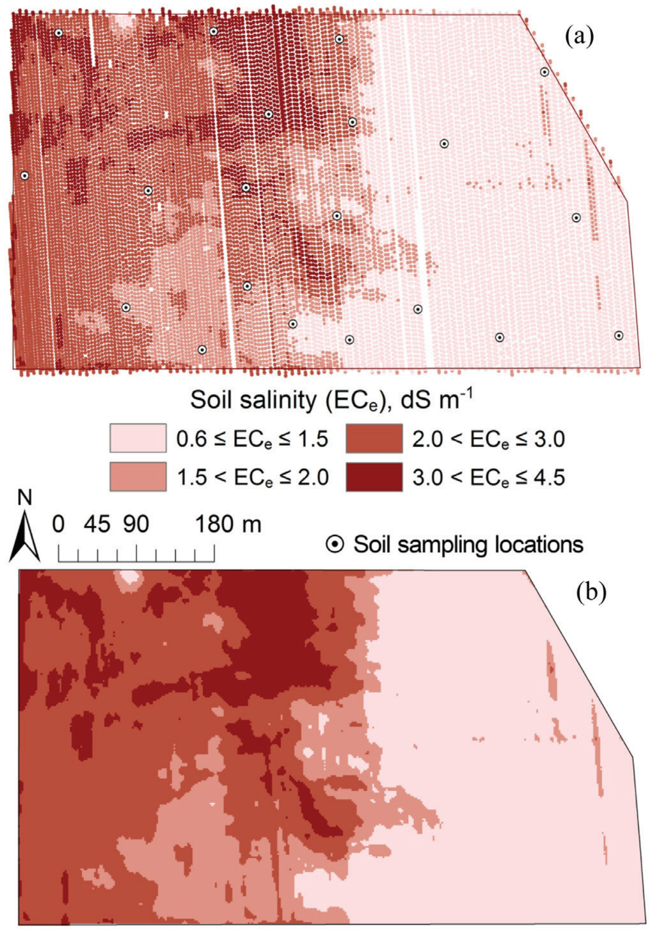

Fig. 12. Soil salinity (a) estimated using Eq. [11] at the 16122 soil apparent electrical conductivity survey locations and (b) interpolated on a 2 × 2 m block support for a 32.4-ha field near San Jacinto, CA.

DATA QUALITY AND PROCESSING

There are four tests that can be conducted to evaluate the reliability of the EC_a survey and target property data. The reliability tests will be discussed from the perspective of the use of EMI measurements of EC_a (i.e., EM_h EC_a and EM_v EC_a). However, the same discussion applies to ER measurements of EC_a, except shallow EC_a measurements with ER (i.e., ideally this is 0–0.75 m, but when using Veris equipment, 0–0.3 m will suffice) correspond to EM_h and deep EC_a measurements with ER (i.e., ideally this is 0–1.5 m, but when using Veris equipment 0–0.9 m will suffice) correspond to EM_v.

The first test is to look at the magnitude of the EC_a measurement. In most instances the EM_v and EM_h EC_a measurements will be greater than 0.05 dS m^{-1}. However, sometimes the measurements are <0.05 dS m^{-1}, which usually occurs for soils that are medium or coarse textured, with very low levels of salinity and/or low water contents. Fine-textured soils with clay contents greater than 30 to 40% will usually have EM_v and EM_h EC_a measurements >0.1 dS m^{-1}. The second test involves the calculation of the ratio EM_h/EM_v. If $EM_h/EM_v < 1$, then the profile is a regular profile, which means that the target property (i.e., EC_e, texture as measured by SP, or water content) increases with depth. If $EM_h/EM_v = 1$, then the profile is a uniform profile, which means that the target property is uniform or oscillates with depth. If $EM_h/EM_v > 1$, then the profile is an inverted profile, which means that the target property decreases with depth. If the depth profile of the target property does not correspond with the EM_h/EM_v ratio, then the EM_h and/or EM_v measurements may be dubious. The third test involves a graph of EM_v vs. EM_h and determination of the correlation coefficient (r) or identification of outliers. If $r \geq 0.8$, then the data are reliable. If $0.5 < r < 0.8$, then possible problems exist with the EC_a data because the upper portion of the soil profile is too dry or the lower portion of the soil profile has (i) a textural discontinuity such as a sand lens, (ii) a shallow water table, or (iii) bed rock. The fourth, and most useful, test involves the use of the DPPC model of Rhoades et al. (1989), which is the ESAP-DPPC module. If entering the soil property values for EC_e, ρ_b, SP, and water content does not result in the calculation of the associated EC_a (the calculated EC_a may not exactly match the observed EC_a, but they should be close) at a given soil sample site, then there is a problem with the data. Unfortunately, the DPPC model only indicates that there is a problem. It does not indicate if the problem is with the EC_a measurement or the soil data (i.e., EC_e, ρ_b, SP, or water content). A limitation of the DPPC model is that it is most suitable for mineral soils and is not applicable to high OM soils.

FARM-, LANDSCAPE-, AND REGIONAL-SCALE SOIL MAPPING

Multiple-field EC_a survey data often exhibit an abrupt change in magnitude across field boundaries, which presents a challenge to the conversion of EC_a to EC_e (or water content or other temporally dynamic target property influenced by management) at spatial extents of hundreds to tens of thousands of hectares (i.e., landscape scale). The abrupt change is caused by various reasons: (i) between-field variation in field average water content due to irrigation method, frequency, and timing; (ii) between-field variation in soil texture; (iii) conditions of the soil surface (e.g., till vs. no-till) due to management practices that affect soil compaction; (iv) surface geometry (i.e., presence or absence of beds and furrows); (v) temperature differences (i.e., EC_a surveys conducted at different times of the year); and (vi) between-field spatial variation in salinity (Corwin and Lesch, 2014).

Calibration models are often used to adjust out an abrupt change. Within similar geomorphological settings, farm- to landscape-scale soil mapping from EC_a–directed soil sampling can be addressed with analysis of covariance (ANOCOVA) linear regression models (Harvey and Morgan, 2009; Corwin and Lesch, 2014). The ANOCOVA models account for changes in the relationships between the target soil property and sensor data due to additive or multiplicative interference of other factors, such as agronomic management (e.g., presence or absence of beds and furrows in a field) or edaphic (e.g., different levels of soil moisture, different texture) factors. In recent years, ANOCOVA models have been tested for the use of EC_a to map soil salinity (Corwin and Lesch, 2014, 2016) and texture (Harvey and Morgan, 2009) over multiple fields (i.e., landscape scale of 1–10 km^2).

Consider the case in which a sensor reading (Xij) is used to map a target soil property (Yij) using calibration location i for a selected group of fields j. The relationship between X and Y is expected to vary between fields. When this relationship changes due to a multiplicative influence (β) resulting from a secondary (nontarget) factor, such as water content or soil tillage, the calibration equation for the sensor readings can be described with a power model Eq. [20], which is the general form of Eq. [9]:

$$Y = \beta X^{\alpha} \varepsilon \qquad [20]$$

where α is the exponential term and ε is a random (multiplicative) error component defined as the ratio between dependent and explanatory terms of the equation (Tian et al., 2013). Once a natural logarithm (ln) transformation is performed on Eq. [20], the multiplicative nature of the relationship becomes additive:

$$\ln\left(Y_{ij}\right) = \ln\left(\beta_j\right) + \alpha \ln\left(X_{ij}\right) + \ln\left(\varepsilon_{ij}\right) \qquad [21]$$

where the intercept parameter (β) is uniquely estimated for each field j, but the slope coefficient (α) is assumed to be constant for a particular group of fields characterized by similar geomorphologic settings. In Eq. [21], ln(ε) is a random (additive) error component. Therefore, Eq. [21] can be parameterized using an OLS approach, provided the assumptions of this type of spatial modeling are respected.

The benefit of using ANOCOVA linear models lies in the fact that once the model is established over a selected number of fields, it can be extended to all the other fields in the farmland of interest by means of an intensive sensor survey and from one to three soil samples that are used to calculate the field-specific ANOCOVA intercept (β).

The definitive studies of regional-scale (i.e., spatial extents covering hundreds of thousands or millions of hectares) mapping of soil properties, particularly salinity, are Lobell et al. (2010) and Scudiero et al. (2015). These studies used multiyear remote imagery (i.e., Landsat 7 and MODIS) in combination with EC_a–directed soil sampling. The remote imagery and other covariates were used with ground-truth measurements of soil salinity from EC_a–directed soil sampling to develop a regression model. Mapping soil properties over regional scales with remote imagery requires significant monetary investment and labor commitment. The following considerations on regional-scale soil sampling and mapping will aid preliminary decision-making:

1. When using remote sensing or other environmental covariates as ancillary predictors, always base their maps on actual ground-truth data. The use of remote and near-ground sensing data, such as vegetation indices calculated from satellite reflectance, must always be calibrated for

each specific geographic zone, type of sensor used, and intended type of application. For example, the same (canopy reflectance) vegetation index (i.e., normalized difference vegetation index) can be used to monitor water stress (texture-related edaphic stress) in certain areas (Scudiero et al., 2014) or soil salinity in a different geographical area (Lobell et al., 2010). Different crop cover can alter the outputs of the prediction models (Scudiero et al., 2015; Zhang et al., 2015), as reflectance properties vary remarkably across plant species because of different phenotypes (e.g., chlorophyll content, canopy size) and different responses to the same stress levels (e.g., stress-tolerant crops vs. nontolerant crops).

2. Regression-based soil mapping, at any scale, requires good representation of the target property in the ground-truth dataset. Over large areas, good spatial coverage is not a necessary requirement as clustered sampling can be employed (Ließ, 2015; Lobell et al., 2010), provided that the sampling locations are selected far enough apart to avoid residual spatial autocorrelation. Ideally, one should select the soil sampling locations across the region of interest according to the frequency statistics of the selected ancillary data. When working at regional scale, however, it is difficult to properly represent such variability using a relatively limited number of soil samples (Ließ, 2015). When dealing with a single sensor, one could select the ground-truth locations by means of a stratified random sampling, where the strata are quantile classes of the selected ancillary variable, as done by Lobell et al. (2010). When accurate data on geomorphologic settings (e.g., soil orders) are available, Ließ (2015) suggested that Jenny's factor model of soil formation should be followed. As the interactions between factors of soil formations influence the output soil property value, one should always consider these interactions within their sampling design: to truly represent an area, it is not enough to guarantee that we are not systematically misrepresenting the density function of a particular predictor, but in addition, all typical landscape positions of the area should be well represented (Ließ, 2015). Additionally, one could employ multiple predictors across the region of interest. In this case, not only the frequency distribution of the different predictors should be considered, but also their correlation structure should be conserved (Clifford et al., 2014; Kidd et al., 2015; Ließ, 2015). This can be done by using principal component analysis on the ancillary data (Lesch, 2005a) or by using methods such as the conditioned Latin hypercube sampling strategy (Minasny and McBratney, 2006). Selection of soil sampling locations, over large areas, that represents the covariates correlation structure and frequency statistics is supported by the ACDC function in the package spsann (Samuel-Rosa et al., 2015) in R (R Development Core Team, 2012).

3. When dealing with regional-scale mapping, one should always consider how to deal with land inaccessibility issues. Reasons for such inaccessibility are several, including issues with access of private land, remoteness (Clifford et al., 2014), and personal safety (Van Zijl et al., 2012; Wu et al., 2014). Recent papers by Clifford et al. (2014), Kidd et al. (2015), and Ließ (2015) addressed the inaccessibility issue in the selection of ground-truth locations for soil mapping. There definitely is a need for flexibility within "real-world" conditions (Kidd et al., 2015). Indeed, once a baseline soil sampling scheme is selected, it can be modified by selecting alternative soil sampling locations that would be less ideal (in terms of the fitness function used in the design optimization), but would allow good representativeness of the predictors frequency statistics and would guarantee accessibility (Clifford et al., 2014).

4. When sampling for ground truth, especially if coarse resolution ancillary data are used (e.g., MODIS reflectance has 250 × 250 m resolution), the within pixel spatial variability should always be addressed (Garrigues et al., 2002). Each target ground-truth pixel or field can be mapped using soil sensor surveys calibrated over a limited amount of soil samples. This strategy will properly characterize subpixel spatial variability and increase the number of ground-truth locations (in comparison with using only soil sample) (Lobell et al., 2010; Scudiero et al., 2015; Wu et al., 2014). Alternatively, when such an approach is not feasible, a nonaligned block sampling design can be used for capturing both small and large variation over large areas (Cobo et al., 2010; Urban, 2002).

The most significant advances in the mapping of soil properties over multiple scales with EC_a–directed soil sampling have been in the area of mapping soil salinity. Different scales require different EC_a– EC_e calibration modeling approaches when mapping soil salinity with EMI (Corwin and Lesch, 2014, 2016; Scudiero et al., 2015). At field scale (<1 km^2) a field-specific regression model (FSR) is appropriate (Corwin and Lesch, 2013):

$$\ln\left(EC_{e,ijk}\right) = \beta_{0,jk} + \beta_{1,jk}\ln\left(EM_{v,ik}\right) + \beta_{2,jk}\ln\left(EM_{h,ik}\right) + \varepsilon_{ijk} \quad [22]$$

At landscape scale (1–10 km^2), an analysis of covariance model (ANOCOVA) is appropriate (Corwin and Lesch, 2014, 2016):

$$\ln\left(EC_{e,ijk}\right) = \beta_{0,jk} + \beta_{1,j}\ln\left(EM_{v,ik}\right) + \beta_{2,j}\ln\left(EM_{h,ik}\right) + \varepsilon_{ijk} \quad [23]$$

At regional scale (10–10^5 km^2), a model based on a vegetative index (e.g., CRSI, NDVI, or EVI) and other covariates influencing a plant's response to salinity is needed (Scudiero et al., 2015):

$$EC_e = \beta_0 + \beta_1(\mathrm{CRSI}) + \beta_2(\mathrm{rain}) + \beta_3(\mathrm{temperature}) + \beta_4(\mathrm{texture}) + \varepsilon \quad [24]$$

where i refers to the soil sample site (i = 1, 2, 3,..., n_k), j refers to the soil sample depth (j = 1, 2, 3,..., p), and k refers to the field (k = 1, 2, 3,..., M).

Considerable progress has also been made in mapping soil texture from EC_a at multiple scales (Neudecker et al., 2001; Vitharana et al., 2008; Harvey and Morgan, 2009; Saey et al., 2009b; Walter et al., 2015). The most notable of these from a regional-scale perspective is Saey et al. (2009b), which mapped texture over 3000 km^2 in Belgium.

ADVANTAGES AND DISADVANTAGES OF EC_a-DIRECTED SOIL SAMPLING

Even though EC_a–directed sampling is widely used for mapping field-scale spatial variability, there are definite advantages, disadvantages, and limitations that determine where and under what conditions it is best used and where there might be concerns for its use. There are three advantages of EC_a–directed sampling. First, it substantially reduces the number of soil samples compared to grid sampling since it uses geospatial EC_a measurements as a surrogate to establish the optimum number and location of sample sites to characterize the range and variability of a target soil property. The reduction in the number of samples greatly reduces labor and cost. Second, EC_a–directed sampling renders quick and reliable results that are statistically tied to ground-truth measurements from soil samples, so there is a direct relationship with salinity or another target property that is highly correlated with EC_a at the study site. Third, EMI is a nondestructive measurement and ER results in minimal soil disturbance.

The disadvantages of EC_a–directed soil sampling do not overshadow the advantages, but are nonetheless worthy of careful consideration. First, the complex interactions of various soil properties and their resulting influences on the EC_a measurement make it a complex measurement that is often difficult to interpret. Second, EC_a–directed sampling requires expensive and technologically sophisticated geophysical and GPS equipment and requires trained personnel to operate it.

There are four major limitations that determine the conditions under which EC_a–directed sampling must be used. First, there must be sufficient water content (i.e., $\geq$70% of field capacity) so continuous conductance pathways are maintained down to the depth of penetration of the geophysical approach used to measure EC_a (i.e., ER or EMI). This may be of particular concern for soils with impermeable layers, dryland soils, or shallow soils above bedrock. Second, the ER approach requires good physical contact between the electrodes and soil surface, and, as such, ER is not generally used in stoney soils or soils with dry surfaces. Third, fields with wide ranging soil textures present a challenge since it may become difficult for the entire field to be at or near field capacity. Fourth, soils that have a shallow water table, impermeable layer, or shallow depth to bedrock are problematic because each of these will interfere with the current flow resulting in spurious EC_a measurements that do not reflect the conductance of the target property (i.e., unless the target property is to determine the depth to a shallow water table, impermeable layer, or bedrock). In instances where a shallow water table, impermeable layer, or shallow depth to bedrock exists, then ER or EMI measurements should be taken so that their depth of penetration is above the water table, impermeable layer, or bedrock.

Acknowledgments

The authors wish to acknowledge the research of numerous scientists over the past three decades that have contributed to the current knowledge and understanding, which culminated in the development of protocols and guidelines for mapping soil spatial variability with EC_a–directed soil sampling. The authors specifically acknowledge the work of Jim Rhoades and Scott Lesch, whose close collaboration with the senior author resulted in the development of the EC_a–directed soil sampling methodology. Also, the diligence, conscientiousness, effort, and technical support of several individuals during the senior author's career who collected the essential field and laboratory data that served as the basis for EC_a–directed soil sampling are acknowledged. These individuals include Kevin Yemoto, Clay Wilkinson, and Harry Forster.

References

Achen, C.H. 1982. Interpreting and using regression. Sage, Beverly Hills, CA. doi:10.4135/9781412984560

Adamchuk, V.I., J.W. Hummel, M.T. Morgan, and S.K. Upadhyaya. 2004. On-the-go soil sensors for precision agriculture. Comput. Electron. Agric. 44:71–91. doi:10.1016/j.compag.2004.03.002

Archie, G.E. 1942. The electrical resistivity log as an aid in determining some reservoir characteristics. Trans. AIME 146:54–62. doi:10.2118/942054-G

Arshad, M.A., and G.M. Coen. 1992. Characterization of soil quality: Physical and chemical criteria. Am. J. Alternative Agric. 7:25–31. doi:10.1017/S0889189300004410

Balanis, C.A. 1989. Advanced engineering electromagnetics. John Wiley and Sons, New York.

Banerjee, S., B.P. Carlin, and A.E. Gelfand. 2014. Hierarchical modeling and analysis for spatial data. CRC Press, Boca Raton, FL.

Barca, E., A. Castrignanò, G. Buttafuoco, D. De Benedetto, and G. Passarella. 2015. Integration of electromagnetic induction sensor data in soil sampling scheme optimization using simulated annealing. Environ. Monit. Assess. 187:422. doi:10.1007/s10661-015-4570-y

Barnes, H.E. 1952. Soil investigation employing a new method of layer-value determination for earth resistivity interpretation. Highway Res. Board Bull. 65:26–36.

Bekele, A., W.H. Hudnall, J.J. Daigle, J.A. Prudente, and M. Wolcott. 2005. Scale dependent variability of soil electrical conductivity by indirect measures of soil properties. J. Terramechs. 42:339–351. doi:10.1016/j.jterra.2004.12.004

Bivand, R., L. Anselin, O. Berke, A. Bernat, M. Carvalho, Y. Chun, C. Dormann, S. Dray, R. Halbersma, and N. Lewin-Koh. 2011. Spdep: Spatial dependence: Weighting schemes, statistics and models. R Package Version 0.5-31. http://CRAN.R-Project.org/package=spdep (accessed 12 Sept. 2016).

Boadu, F.K., and B. Seabrook. 2006. Effect of clay and salinity on the spectral electrical response of soils. J. Environ. Eng. Geophys. 11:161–170. doi:10.2113/JEEG11.3.161

Borchers, B., T. Uram, and J.M.H. Hendrickx. 1997. Tikhonov regularization of electrical conductivity depth profiles in field soils. Soil Sci. Soc. Am. J. 61:1004–1009. doi:10.2136/sssaj1997.03615995006100040002x

Bourgault, G., A.G. Journel, J.D. Rhoades, D.L. Corwin, and S.M. Lesch. 1997. Geostatistical analysis of a soil salinity data set. In: D.L. Sparks, editor, Advances in Agronomy. Academic Press, San Diego, CA. p. 241–292.

Bouma, J. 1989. Using soil survey data for quantitative land evaluation. Adv. Soil Sci. 9:177–213. doi:10.1007/978-1-4612-3532-3_4

Brevik, E.C., and T.E. Fenton. 2004. The effect of changes in bulk density on soil electrical conductivity as measured with the Geonics® EM-38. Soil Surv. Horiz. 45(3):96–102. doi:10.2136/sh2004.3.0096

Brevik, E.C., T.E. Fenton, and R. Horton. 2004. Effect of daily soil temperature fluctuations on soil electrical conductivity as measured with the Geonics® EM-38. Precis. Agric. 5:145–152. doi:10.1023/B:PRAG.0000022359.79184.92

Brus, D. 2015. Balanced sampling: A versatile sampling approach for statistical soil surveys. Geoderma 253–254:111–121. doi:10.1016/j.geoderma.2015.04.009

Brus, D.J., and J.J. DeGruijter. 1993. Design-based versus model-based estimates of spatial means: Theory and application in environmental soil science. Environmetrics 4:123–152. doi:10.1002/env.3170040202

Brus, D.J., and G.B. Heuvelink. 2007. Optimization of sample patterns for universal kriging of environmental variables. Geoderma 138:86–95. doi:10.1016/j.geoderma.2006.10.016

Burgess, T., and R. Webster. 1984. Optimal sampling strategies for mapping soil types. I. distribution of boundary spacings. J. Soil Sci. 35:641–654. doi:10.1111/j.1365-2389.1984.tb00621.x

Burgess, T., R. Webster, and A. McBratney. 1981. Optimal interpolation and isarithmic mapping of soil properties. IV. Sampling strategy. J. Soil Sci. 32:643–659. doi:10.1111/j.1365-2389.1981.tb01737.x

Cannon, M.E., R.C. McKenzie, and G. Lachapelle. 1994. Soil-salinity mapping with electromagnetic induction and satellite-based navigation methods. Can. J. Soil Sci. 74(3):335–343. doi:10.4141/cjss94-046

Carter, L.M., J.D. Rhoades, and J.H. Chesson. 1993. Mechanization of soil salinity assessment for mapping. ASAE Paper 931557. ASAE, St. Joseph, MI, USA.

Castrignanò, A., F. Morari, C. Fiorentino, C. Pagliarin, and S. Brenna. 2008. Constrained optimization of spatial sampling in skeletal soils using EMI data and continuous simulated annealing. In: 1st Global Workshop on High Resolution Digital Soil Sensing & Mapping, Sydney, Australia. 5–8 Feb. 2008.

Cliff, A.D., and J.K. Ord. 1981. Spatial processes: Models & applications. Pion, London, UK.

Clifford, D., J.E. Payne, M. Pringle, R. Searle, and N. Butler. 2014. Pragmatic soil survey design using flexible latin hypercube sampling. Comput. Geosci. 67:62–68. doi:10.1016/j.cageo.2014.03.005

Cobo, J.G., G. Dercon, T. Yekeye, L. Chapungu, C. Kadzere, A. Murwira, R. Delve, and G. Cadisch. 2010. Integration of mid-infrared spectroscopy and geostatistics in the assessment of soil spatial variability at landscape level. Geoderma 158:398–411. doi:10.1016/j.geoderma.2010.06.013

Cook, P.G., and S. Kilty. 1992. A helicopter-borne electromagnetic survey to delineate groundwater recharge rates. Water Resour. Res. 28(11):2953–2961. doi:10.1029/92WR01560

Corwin, D.L. 2005. Geospatial measurements of apparent soil electrical conductivity for characterizing soil spatial variability. In: J. Álvarez-Benedi and R. Muñoz-Carpena, editors, Soil-water-solute process characterization. CRC Press, Boca Raton, FL. p. 639–672.

Corwin, D.L. 2008. Past, present, and future trends of soil electrical conductivity measurement using geophysical methods. In: B.J. Allred, J.J. Daniels, and M.R. Ehsani, editors, Handbook of agricultural geophysics. CRC Press, Boca Raton, FL. p. 17–44.

Corwin, D.L., and H.R. Ahmad. 2015. Spatio-temporal impacts of dairy lagoon water reuse on soil: Heavy metals and salinity. Environ. Sci. Process. Impacts 17:1731–1748. doi:10.1039/C5EM00196J

Corwin, D.L., M.L.K. Carrillo, P.J. Vaughan, J.D. Rhoades, and D.G. Cone. 1999. Evaluation of GIS-linked model of salt loading to groundwater. J. Environ. Qual. 28:471–480. doi:10.2134/jeq1999.00472425002800020012x

Corwin, D.L., S.R. Kaffka, J.W. Hopmans, Y. Mori, S.M. Lesch, and J.D. Oster. 2003b. Assessment and field-scale mapping of soil quality properties of a saline-sodic soil. Geoderma 114(3–4):231–259. doi:10.1016/S0016-7061(03)00043-0

Corwin, D.L., and S.M. Lesch. 2003. Application of soil electrical conductivity to precision agriculture: Theory, principles and guidelines. Agron. J. 95(3):455–471. doi:10.2134/agronj2003.0455

Corwin, D.L., and S.M. Lesch. 2005a. Apparent soil electrical conductivity measurements in agriculture. Comput. Electron. Agric. 46(1–3):11–43. doi:10.1016/j.compag.2004.10.005

Corwin, D.L., and S.M. Lesch. 2005b. Characterizing soil spatial variability with apparent soil electrical conductivity: I. Survey protocols. Comput. Electron. Agric. 46(1–3):103–133. doi:10.1016/j.compag.2004.11.002

Corwin, D.L., and S.M. Lesch. 2005c. Characterizing soil spatial variability with apparent soil electrical conductivity: Part II. Case study. Comput. Electron. Agric. 46:135–152. doi:10.1016/j.compag.2004.11.003

Corwin, D.L., and S.M. Lesch. 2010. Delineating site-specific management units with proximal sensors. In: M. Oliver, editor, Geostatistical applications in precision agriculture. Springer, New York. p. 139–165. doi:10.1007/978-90-481-9133-8_6

Corwin, D.L., and S.M. Lesch. 2013. Protocols and guidelines for field-scale measurement of soil salinity distribution with EC_a–directed soil sampling. J. Environ. Eng. Geophys. 18(1):1–25. doi:10.2113/JEEG18.1.1

Corwin, D.L., and S.M. Lesch. 2014. A simplified regional-scale electromagnetic induction–salinity calibration model using ANOCOVA modeling techniques. Geoderma 230-231:288–295. doi:10.1016/j.geoderma.2014.03.019

Corwin, D.L., and S.M. Lesch. 2016. Validation of the ANOCOVA model for regional-scale EC_a to EC_e calibration. Soil Use Manage. doi:10.1111/sum.12262

Corwin, D.L., S.M. Lesch, J.D. Oster, and S.R. Kaffka. 2006. Monitoring management-induced spatio-temporal changes in soil quality with soil sampling directed by apparent soil electrical conductivity. Geoderma 131:369–387. doi:10.1016/j.geoderma.2005.03.014

Corwin, D.L., S.M. Lesch, E. Segal, T.H. Skaggs, and S.A. Bradford. 2010. Comparison of sampling strategies for characterizing spatial variability with apparent soil electrical conductivity directed soil sampling. J. Environ. Eng. Geophys. 15:147–162. doi:10.2113/JEEG15.3.147

Corwin, D.L., S.M. Lesch, P.J. Shouse, R. Soppe, and J.E. Ayars. 2003a. Identifying soil properties that influence cotton yield using soil sampling directed by apparent soil electrical conductivity. Agron. J. 95(2):352–364. doi:10.2134/agronj2003.0352

Corwin, D.L., and J.D. Rhoades. 1982. An improved technique for determining soil electrical conductivity–depth relations from above-ground electromagnetic measurements. Soil Sci. Soc. Am. J. 46:517–520. doi:10.2136/sssaj1982.03615995004600030014x

Dane, J.H., and G.C. Topp, editors. 2002. Methods of soil analysis. Part 4. Physical methods. SSSA Book Ser. 5. SSSA, Madison, WI.

Debba, P., F. Van Ruitenbeek, F. Van Der Meer, E. Carranza, and A. Stein. 2005. Optimal field sampling for targeting minerals using hyperspectral data. Remote Sens. Environ. 99:373–386. doi:10.1016/j.rse.2005.05.005

Doolittle, J.A., and E.C. Brevik. 2014. The use of electromagnetic induction techniques in soils studies. Geoderma 223-225:33–45. doi:10.1016/j.geoderma.2014.01.027

Doolittle, J., A. Stuebe, A. Price, and E. Kelly. 2002. Mapping bedrock depths with electromagnetic induction in Costilla County, Colorado. Soil Surv. Horiz. 43(1):14–21. doi:10.2136/sh2002.1.0014

Doolittle, J.A., K.A. Sudduth, N.R. Kitchen, and S.J. Indorante. 1994. Estimating depths to claypans using electromagnetic induction methods. J. Soil Water Conserv. 49(6):572–575.

Doran, J.W., and T.B. Parkin. 1994. Defining and assessing soil quality. In: J.W. Doran, D.C. Coleman, D.F., Bedzicek, and B.A. Stewart, editors, Defining soil quality for a sustainable environment. SSSA Special Publ. 35. SSSA, Madison, WI. p. 3–22.

Doran, J.W., and T.B. Parkin. 1996. Quantitative indicators of soil quality: A minimum data set. In: J.W. Doran and A.J. Jones, editors, Methods for assessing soil quality. SSSA Spec. Publ. 49. SSSA, Madison, WI. p. 25–38. doi:10.2136/sssaspecpub49.c2

Efron, B., and G. Gong. 1983. A leisurely look at the bootstrap, the jackknife, and cross-validation. Am. Stat. 37:36–48.

Fenton, T.E., and M.A. Lauterbach. 1999. Soil map unit composition and scale of mapping related to interpretations for precision soil and crop management in Iowa. In: P.C. Robert, R.H. Rust, W.E. Larson, editors, Proc. 4th International Conference on Precision Agriculture, St. Paul, MN, 19–22 July 1998. ASA, CSSA, and SSSA, Madison, WI. p. 239–251.

Fitzgerald, G.J., S.M. Lesch, E.M. Barnes, and W.E. Luckett. 2006. Directed sampling using remote sensing with a response surface sampling design for site-specific agriculture. Comput. Electron. Agric. 53:98–112. doi:10.1016/j.compag.2006.04.003

Freeland, R.S., R.E. Yoder, J.T. Ammons, and L.L. Leonard. 2002. Mobilized surveying of soil conductivity using electromagnetic induction. Appl. Eng. Agric. 18(1):121–126. doi:10.13031/2013.7701

Garrigues, S., D. Allard, M. Weiss, F. Baret, S. Marni, and H. Jeanjean. 2002. Influence of spatial heterogeneity and scaling on leaf area index estimates from remote sensing data. In: J.A. Sobrino, editor, Recent advances in quantitative remote sensing. Univ. de València, Valencia. p. 199.

Gavlak, R.G., D.A. Horneck, R.O. Miller, and J. Kotuby-Amacher. 2003. Soil, plant. and water reference methods for the western region. 2nd ed. WCC-103 Publ., WREP-125.

Gebbers, R., E. Lück, M. Dabas, and H. Domsch. 2009. Comparison of instruments for geoelectrical soil mapping at the field scale. Near Surf. Geophys. 7(3):179–190.

Gotway, C.A., R.B. Ferguson, G.W. Hergert, and T.A. Peterson. 1996. Comparison of kriging and inverse-distance methods for mapping soil parameters. Soil Sci. Soc. Am. J. 60:1237–1247. doi:10.2136/sssaj1996.03615995006000040040x

Greenhouse, J.P., and D.D. Slaine. 1983. The use of reconnaissance electromagnetic methods to map contaminant migration. Ground Water Monit. Rev. 3(2):47–59. doi:10.1111/j.1745-6592.1983.tb01199.x

Guo, Y., Z. Shi, J. Huang, L. Zhou, Y. Zhou, and L. Wang. 2015. Characterization of field scale soil variability using remotely and proximally sensed data and response surface method. Stochastic Environ. Res. Risk Assess. doi:10.1007/s00477-015-1135-0

Hanna, A.Y., P.W. Harlan, and D.T. Lewis. 1982. Soil available water as influenced by landscape position and aspect. Agron. J. 74(6):999–1004. doi:10.2134/agronj1982.00021962007400060016x

Harvey, O.R., and C.L. Morgan. 2009. Predicting regional-scale soil variability using a single calibrated apparent soil electrical conductivity model. Soil Sci. Soc. Am. J. 73:164–169. doi:10.2136/sssaj2008.0074

Haskard, K.A., B.R. Cullis, and A.P. Verbyla. 2007. Anisotropic Matérn correlation and spatial prediction using REML. J. Agric. Biol. Environ. Stat. 12:147–160. doi:10.1198/108571107X196004

Heil, K., and U. Schmidhalter. 2012. Characterisation of soil texture variability using the apparent soil electrical conductivity at a highly variable site. Comput. Geosci. 39:98–110. doi:10.1016/j.cageo.2011.06.017

Heil, K., and U. Schmidhalter. 2015. Comparison of the EM38 and EM38-MK2 electromagnetic induction-based sensors for spataial soil analysis at field scale. Comput. Electron. Agric. 110:267–280. doi:10.1016/j.compag.2014.11.014

Hendrickx, J.M.H., B. Borchers, D.L. Corwin, S.M. Lesch, A.C. Hilgendorf, and J. Schlue. 2002b. Inversion of soil conductivity profiles from electromagnetic induction measurements: Theory and experimental verification. Soil Sci. Soc. Am. J. 66:673–685. doi:10.2136/sssaj2002.6730

Hendrickx, J.M.H., B. Das, D.L. Corwin, J.M. Wraith, and R.G. Kachanoski. 2002a. Indirect measurement of solute concentration. In: J.H. Dane and G.C. Topp, editors, Methods of soil analysis. Part 4. physical methods. SSSA Book Ser. 5. SSSA, Madison, WI. p. 1274–1306. doi:10.2136/sssabookser5.4.c54

Hengl, T. 2006. Finding the right pixel size. Comput. Geosci. 32:1283–1298. doi:10.1016/j.cageo.2005.11.008

Hengl, T., D.G. Rossiter, and A. Stein. 2003. Soil sampling strategies for spatial prediction by correlation with auxiliary maps. Aust. J. Soil Res. 41:1403–1422. doi:10.1071/SR03005

Heuvelink, G.B.M. 1998. Error propagation in environmental modelling with GIS. CRC Press, Padstow, UK.

Isaaks, E.H., and R.M. Srivastava. 1989. Applied geostatistics. Oxford Univ. Press, New York, NY, USA.

Islam, M.M., E. Meerschman, T. Saey, P. De Smedt, E. Van De Vijver, S. Delefortrie, and M. Van Meirvenne. 2014. Characterizing compaction variability with an electromagnetic induction sensor in a puddled paddy rice field. Soil Sci. Soc. Am. J. 78(2):579–588. doi:10.2136/sssaj2013.07.0289

Jansen, J., J. Anklam, C. Goodwin, and A. Roof. 1993. Electromagnetic induction and seismic refraction surveys to detect bedrock pinnacles. In: Applied karst geology. Balkema, Rotterdam. p. 115–122.

Jaynes, D.B. 1996. Mapping the areal distribution of soil parameters with geophysical techniques. In: D.L. Corwin and K. Loague, editors, Applications of GIS to the modeling of non-point source pollutants in the vadose zone. SSSA Spec. Publ. 48. SSSA, Madison, WI. p. 205–216. doi:10.2136/sssaspecpub48.c12

Jaynes, D.B., J.M. Novak, T.B. Moorman, and C.A. Cambardella. 1995. Estimating herbicide partition coefficients from electromagnetic induction measurements. J. Environ. Qual. 24:36–41. doi:10.2134/jeq1995.00472425002400010005x

Jaynes, D.B., T.S. Colvin, and J. Ambuel. 1993. Soil type and crop yield determinations from ground conductivity surveys. ASAE Paper 933552. ASAE, St. Joseph, MI.

Johnson, C., K.M. Eskridge, and D. Corwin. 2005. Apparent soil electrical conductivity: Applications for designing and evaluating field-scale experiments. Comput. Electron. Agric. 46:181–202. doi:10.1016/j.compag.2004.12.001

Kachanoski, R.G., E.G. Gregorich, and I.J. Van-Wesenbeeck. 1988. Estimating spatial variations of soil water content using noncontacting electromagnetic inductive methods. Can. J. Soil Sci. 68:715–722. doi:10.4141/cjss88-069

Kidd, D., B. Malone, A. McBratney, B. Minasny, and M. Webb. 2015. Operational sampling challenges to digital soil mapping in Tasmania, Australia. Geoderma Regional 4:1–10. doi:10.1016/j.geodrs.2014.11.002

Kitchen, N.R., K.A. Sudduth, and S.T. Drummond. 1996. Mapping of sand deposition from 1993 Midwest floods with electromagnetic induction measurements. J. Soil Water Conserv. 51(4):336–340.

Klestra, E.J., and J.K. Bartz. 1996. Quality assurance and quality control. In: D.L. Sparks, editor, Methods of soil analysis. Part 3. Chemical methods. SSSA Book Ser. 5. SSSA, Madison, WI. p. 19–48. doi:10.2136/sssabookser5.3.c2

Kravchenko, A.N., and D.G. Bullock. 1999. A comparative study of interpolation methods for mapping soil properties. Agron. J. 91:393–400. doi:10.2134/agronj1999.00021962009100030007x

Kravchenko, A.N., G.A. Bollero, R.A. Omonode, and D.G. Bullock. 2002. Quantitative mapping of soil drainage classes using topographical data and soil electrical conductivity. Soil Sci. Soc. Am. J. 66:235–243. doi:10.2136/sssaj2002.2350

Lamb, D.W., A. Mitchell, and G. Hyde. 2005. Vineyard trellising with steel posts distorts data from EM soil surveys. Aust. J. Grape Wine Res. 11:24–32. doi:10.1111/j.1755-0238.2005.tb00276.x

Lark, R.M., S.R. Kaffka, and D.L. Corwin. 2003. Multiresolution analysis of data of electrical conductivity of soil using wavelets. J. Hydrol. 272:276–290. doi:10.1016/S0022-1694(02)00271-8

Larson, W.E., and F.J. Pierce. 1991. Conservation and enhancement of soil quality. In: J. Dumanski, editor, Proceedings of the International Workshop on Evaluation for Sustainable Land Management in the Developing World. Vol. 2.Technical Papers. Chaning Rai, Thailand, 15–21 Sept. 1990. Int. Board Soil Res. Manage., Bangkok, Thailand. p. 175–203.

Larson, W.E., and F.J. Pierce. 1994. The dynamics of soil quality as a measure of sustainable management. In: J.W. Doran, D.C. Coleman, D.F. Bedzicek, and B.A. Stewart, editors, Defining soil quality for a sustainable environment. SSSA Spec. Publ. 35. SSSA, Madison, WI. p. 37–51. doi:10.2136/sssaspecpub35.c3

Laslett, G.M., A.B. McBratney, P.J. Pahl, and M.F. Hutchinson. 1987. Comparison of several spatial prediction methods for soil pH. J. Soil Sci. 38:325–341. doi:10.1111/j.1365-2389.1987.tb02148.x

Leenaers, H., J.P. Okx, and P.A. Burrough. 1990. Comparison of spatial prediction methods for mapping floodplain soil pollution. Catena 17:535–550. doi:10.1016/0341-8162(90)90028-C

Lesch, S.M. 2005a. Sensor-directed response surface sampling designs for characterizing spatial variation in soil properties. Comput. Electron. Agric. 46(1–3):153–179. doi:10.1016/j.compag.2004.11.004

Lesch, S.M. 2012. Statistical models for the prediction of field-scale and spatial salinity patterns from soil conductivity survey data. In: W.W. Wallender and K.K. Tanji, editors, Agricultural salinity assessment and management. ASCE, Reston, VA. p. 461–482.

Lesch, S.M., and D.L. Corwin. 2003. Using the dual-pathway parallel conductance model to determine how different soil properties influence conductivity survey data. Agron. J. 95:365–379. doi:10.2134/agronj2003.0365

Lesch, S.M., and D.L. Corwin. 2008. Prediction of spatial soil property information from ancillary sensor data using ordinary linear regression: Model derivations, residual assumptions and model validation tests. Geoderma 148:130–140. doi:10.1016/j.geoderma.2008.09.014

Lesch, S.M., D.J. Strauss, and J.D. Rhoades. 1995a. Spatial prediction of soil salinity using electromagnetic induction techniques. 1. Statistical prediction models: A comparison of multiple linear regression and cokriging. Water Resour. Res. 31:373–386. doi:10.1029/94WR02179

Lesch, S.M., D.J. Strauss, and J.D. Rhoades. 1995b. Spatial prediction of soil salinity using electromagnetic induction techniques. 2.Anefficient spatial sampling algorithm suitable for multiple linear regression model identification and estimation. Water Resour. Res. 31:387–398. doi:10.1029/94WR02180

Lesch, S.M., D.L. Corwin, and D.A. Robinson. 2005. Apparent soil electrical conductivity mapping as an agricultural management tool in arid zone soils. Comput. Electron. Agric. 46:351–378. doi:10.1016/j.compag.2004.11.007

Lesch, S.M., J.D. Rhoades, and D.L. Corwin. 2000. ESAP-95 version 2.10R: User and tutorial guide, Research Rep. 146. USDA-ARS, US Salinity Laboratory, Riverside, CA.

Lesch, S.M., J.D. Rhoades, L.J. Lund, and D.L. Corwin. 1992. Mapping soil salinity using calibrated electromagnetic measurements. Soil Sci. Soc. Am. J. 56:540–548. doi:10.2136/sssaj1992.03615995005600020031x

Lesch, S.M., J. Herrero, and J.D. Rhoades. 1998. Monitoring for temporal changes in soil salinity using electromagnetic induction techniques. Soil Sci. Soc. Am. J. 62:232–242. doi:10.2136/sssaj1998.03615995006200010030x

Li, Y., S. Zhou, C. Wu, L. Feng, and H. Li. 2007. Optimised spatial sampling scheme for soil electrical conductivity based on variance quad-tree (VQT) method. Agric. Sci. China 6:1463–1471. doi:10.1016/S1671-2927(08)60009-7

Ließ, M. 2015. Sampling for regression-based digital soil mapping: Closing the gap between statistical desires and operational applicability. Spat. Stat. 13:106–122. doi:10.1016/j.spasta.2015.06.002

Littell, R.C., W.W. Stroup, G.A. Milliken, R.D. Wolfinger, and O. Schabenberger. 2006. SAS for mixed models. SAS institute Inc., Cary, NC, USA.

Lobell, D.B., S.M. Lesch, D.L. Corwin, M.G. Ulmer, K.A. Anderson, D.J. Potts, J.A. Doolittle, M.R. Matos, and M.J. Baltes. 2010. Regional-scale assessment of soil salinity in the Red River Valley using multi-year MODIS EVI and NDVI. J. Environ. Qual. 39:35–41. doi:10.2134/jeq2009.0140

Lund, E.D., C.D. Chrissty, and P.E. Drummond. 1999. Applying soil electrical conductivity to precision agriculture. In P.C. Robert, R.H. Rust, and W.E. Larson, editors, Proceedings of the Fourth International Conference on Precision Agriculture, St. Paul, MN, 19–22 July 1998. ASA, CSSA, and SSSA, Madison, WI. p. 1089–1100.

McBratney, A.B., T.F.A. Bishop, and I.S. Teliatnikov. 2000. Two soil profile reconstruction techniques. Geoderma 97:209–221. doi:10.1016/S0016-7061(00)00039-2

McBride, R.A., A.M. Gordon, and S.C. Shrive. 1990. Estimating forest soil quality from terrain measurements of apparent electrical conductivity. Soil Sci. Soc. Am. J. 54:290–293. doi:10.2136/sssaj1990.03615995005400010047x

Metropolis, N., A. Rosembluth, M. Rosembluth, and A. Teller. 1953. Equation of state calculations by very fast computing machines. J. Chem. Phys. 21:1087–1092. doi:10.1063/1.1699114

Minasny, B., A.B. McBratney, and D.J. Walvoort. 2007. The variance quadtree algorithm: Use for spatial sampling design. Comput. Geosci. 33:383–392. doi:10.1016/j.cageo.2006.08.009

Minasny, B., and A.B. McBratney. 2006. A conditioned Latin hypercube method for sampling in the presence of ancillary information. Comput. Geosci. 32:1378–1388. doi:10.1016/j.cageo.2005.12.009

Minasny, B., and A.B. McBratney. 2007. Spatial prediction of soil properties using EBLUP with the Matérn covariance function. Geoderma 140:324–336. doi:10.1016/j.geoderma.2007.04.028

Mitchell, A. 2005. The ESRI guide to GIS analysis. Vol. 2. Spatial measurements and statistics. ESRI Press, Redlands, CA.

Myers, R.H., D.C. Montgomery, and C.M. Anderson-Cook. 2009. Response surface methodology: Process and product optimization using designed experiments. John Wiley and Sons, New York.

Nelson, M., T. Bishop, J. Triantafilis, and I. Odeh. 2011. An error budget for different sources of error in digital soil mapping. Eur. J. Soil Sci. 62:417–430. doi:10.1111/j.1365-2389.2011.01365.x

Neudecker, E., U. Schmidhalter, C. Sperl, and T. Selige. 2001. Site-specific soil mapping by electromagnetic induction. In: G. Grenier and S. Blackmore, editors, Proceedings of the 3rd European Conference on Precision Agriculture. Agro Montpellier, Montpellier, France. p. 271–276.

Nielsen, D.R., J.W. Biggar, and K.T. Erh. 1973. Spatial variability of field-measured soil-water properties. Hilgardia 42(7):215–259. doi:10.3733/hilg.v42n07p215

O'Brien, R.M. 2007. A caution regarding rules of thumb for variance inflation factors. Qual. Quant. 41:673–690. doi:10.1007/s11135-006-9018-6

Peters, D.B. 1965. Water availability. In: C.A. Black, D.D. Evans, J.L. White, L.E. Ensminger, and F.E. Clark, editors, Methods of soil analysis. Part 1. Physical and mineralogical properties, including statistics of measurement and sampling. Agronomy Monogr. 9. ASA, Madison, WI. p. 279–285. doi:10.2134/agronmonogr9.1.c19

Peterson, R.G., and L.D. Calvin. 1996. Sampling. In: D.L. Sparks, editor, Methods of soil analysis. Part 3. Chemical methods. SSSA Book Ser. 5. SSSA, Madison, WI. p. 1–17. doi:10.2136/sssabookser5.3.c1

R Development Core Team. 2012. R: A language and environment for statistical computing. R Foundation for Statistical Computing, Vienna, Austria.

Rhoades, J.D. 1981. Determining leaching fraction from field measurements of soil electrical conductivity. Agric. Water Manage. 3:205–215. doi:10.1016/0378-3774(81)90004-4

Rhoades, J.D. 1992. Instrumental field methods of salinity appraisal. In: G.C. Topp, W.D. Reynolds, and R.E. Green, editors, Advances in measurement of soil physical properties: Bringing theory into practice. SSSA Spec. Pub. 30. SSSA, Madison, WI. p. 231–248.

Rhoades, J.D. 1993. Electrical conductivity methods for measuring and mapping soil salinity. In: D.L. Sparks, editor, Advances in Agronomy. Vol. 49. Academic Press, San Diego, CA. p. 201–251. doi:10.1016/S0065-2113(08)60795-6

Rhoades, J.D. 1996. Salinity: Electrical conductivity and total dissolved salts. In: D.L. Sparks, editor, Methods of soil analysis. Part 3. Chemical methods. SSSA Book Ser. 5. SSSA, Madison, WI. p. 417–435. doi:10.2136/sssabookser5.3.c14

Rhoades, J.D., and D.L. Corwin. 1981. Determining soil electrical conductivity–depth relations using an inductive electromagnetic soil conductivity meter. Soil Sci. Soc. Am. J. 45:255–260. doi:10.2136/sssaj1981.03615995004500020006x

Rhoades, J.D., D.L. Corwin, and S.M. Lesch. 1999b. Geospatial measurements of soil electrical conductivity to assess soil salinity and diffuse salt loading from irrigation. In: D.L. Corwin, K. Loague, and T.R. Ellsworth, editors, Assessment of non-point source pollution in the vadose zone. Geophysical Monogr. 108. AGU, Washington, DC. p. 197–215. doi:10.1029/GM108p0197

Rhoades, J.D., F. Chanduvi, and S. Lesch. 1999a. Soil salinity assessment: Methods and interpretation of electrical conductivity measurements. FAO Irrigation and Drainage Paper 57. FAO, Rome.

Rhoades, J.D., S.M. Lesch, R.D. LeMert, and W.J. Alves. 1997. Assessing irrigation/drainage/salinity management using spatially referenced salinity measurements. Agric. Water Manage. 35:147–165. doi:10.1016/S0378-3774(97)00017-6

Rhoades, J.D., N.A. Manteghi, P.J. Shouse, and W.J. Alves. 1989. Soil electrical conductivity and soil salinity: New formulations and calibrations. Soil Sci. Soc. Am. J. 53:433–439. doi:10.2136/sssaj1989.03615995005300020020x

Rhoades, J.D., P.A.C. Raats, and R.J. Prather. 1976. Effects of liquid-phase electrical conductivity, water content, and surface conductivity on bulk soil electrical conductivity. Soil Sci. Soc. Am. J. 40:651–655. doi:10.2136/sssaj1976.03615995004000050017x

Rhoades, J.D., P.J. Shouse, W.J. Alves, N.M. Manteghi, and S.M. Lesch. 1990. Determining soil salinity from soil electrical conductivity using different models and estimates. Soil Sci. Soc. Am. J. 54:46–54. doi:10.2136/sssaj1990.03615995005400010007x

Roberts, E.A., R.L. Sheley, and R.L. Lawrence. 2004. Using sampling and inverse distance weighted modeling for mapping invasive plants. West. N. Am. Nat. 64:312–323.

Robinson, D.A., I. Lebron, S.M. Lesch, and P. Shouse. 2004. Minimizing drift in electrical conductivity measurements in high temperature environments using the EM-38. Soil Sci. Soc. Am. J. 68:339–345. doi:10.2136/sssaj2004.3390

Rodrigues, F., R. Bramley, and D. Gobbett. 2015. Proximal soil sensing for precision agriculture: Simultaneous use of electromagnetic induction and gamma radiometrics in contrasting soils. Geoderma 243–244:183–195. doi:10.1016/j.geoderma.2015.01.004

Saey, T., D. Simpson, H. Vermeersch, L. Cockx, and M. Van Meirvenne. 2009a. Comparing the EM38DD and DUALEM-21S sensors for depth-to-clay mapping. Soil Sci. Soc. Am. J. 73(1):7–12. doi:10.2136/sssaj2008.0079

Saey, T., M. Van Meirvenne, H. Vermeersch, N. Ameloot, and L. Cockx. 2009b. A pedotransfer function to evaluate the soil profile textural heterogeneity using proximally sensed apparent electrical conductivity. Geoderma 150(3–4):389–395. doi:10.1016/j.geoderma.2009.02.024

Samuel-Rosa, A., G. Heuvelink, G. Vasques, and L. Anjos. 2015. Spsann-optimization of sample patterns using spatial simulated annealing. In: Spsann-optimization of sample patterns using spatial simulated annealing. EGU general Assembly Conference Abstract 7780. EGU, Vienna, Austria.

Schabenberger, O., and C.A. Gotway. 2004. Statistical methods for spatial data analysis. Chapman & Hall/CRC, Boca Raton, FL.

Schumann, A.W., and Q.U. Zaman. 2003. Mapping water table depth by electromagnetic induction. Appl. Eng. Agric. 19(6):675–688. doi:10.13031/2013.15663

Scudiero, E., D.L. Corwin, and T.H. Skaggs. 2015. Regional-scale soil salinity assessment using Landsat ETM+ canopy reflectance. Remote Sens. Environ. 169:335–343. doi:10.1016/j.rse.2015.08.026

Scudiero, E., R. Deiana, P. Teatini, G. Cassiani, and F. Morari. 2011. Constrained optimization of spatial sampling in salt contaminated coastal farmland using EMI and continuous simulated annealing. Procedia Environ. Sci. 7:234–239. doi:10.1016/j.proenv.2011.07.041

Scudiero, E., P. Teatini, D.L. Corwin, R. Deiana, A. Berti, and F. Morari. 2013. Delineation of site-specific management units in a saline region at the Venice lagoon margin, Italy, using soil reflectance and apparent electrical conductivity. Comput. Electron. Agric. 99:54–64. doi:10.1016/j.compag.2013.08.023

Scudiero, E., P. Teatini, D.L. Corwin, N.D. Ferro, G. Simonetti, and F. Morari. 2014. Spatiotemporal response of maize yield to edaphic and meteorological conditions in a saline farmland. Agron. J. 106:2163–2174. doi:10.2134/agronj14.0102

Serrano, J., S. Shahidian, and J.M. da Silva. 2014. Spatial and temporal patterns of apparent electrical conductivity: DUALEM vs. Veris sensors for monitoring soil properties. Sensors (Basel Switzerland) 14:10024–10041. doi:10.3390/s140610024

Shapiro, S.S., and M.B. Wilk. 1965. An analysis of variance test for normality (complete samples). Biometrika 52:591–611. doi:10.1093/biomet/52.3-4.591

Sheets, K.R., and J.M.H. Hendrickx. 1995. Non-invasive soil water content measurement using electromagnetic induction. Water Resour. Res. 31:2401–2409. doi:10.1029/95WR01949

Sparkes, D., K. Jaggard, S. Ramsden, and R. Scott. 1998. The effect of field margins on the yield of sugar beet and cereal crops. Ann. Appl. Biol. 132:129–142. doi:10.1111/j.1744-7348.1998.tb05190.x

Sparks, D.L., editor. 1996. Methods of soil analysis. Part 3. Chemical methods. SSSA Book Ser. 5. SSSA, Madison, WI.

Stiven, G.A., and M.A. Khan. 1966. Saturation percentage as a measure of soil texture in the Lower Indus Basin. J. Soil Sci. 17(2):255–273. doi:10.1111/j.1365-2389.1966.tb01471.x

Sudduth, K.A., S.T. Drummond, and N.R. Kitchen. 2001. Accuracy issues in electromagnetic induction sensing of soil electrical conductivity for precision agriculture. Comput. Electron. Agric. 31:239–264. doi:10.1016/S0168-1699(00)00185-X

Sudduth, K.A., N.R. Kitchen, G.A. Bollero, D.G. Bullock, and W.J. Wiebold. 2003. Comparison of electromagnetic induction and direct sensing of soil electrical conductivity. Agron. J. 95:472–482. doi:10.2134/agronj2003.0472

Sudduth, K.A., N.R. Kitchen, and S.T. Drummond. 1999. Soil conductivity sensing on claypan soils: Comparison of electromagnetic induction and direct methods. In: P.C. Robert, R.H. Rust, and W.E. Larson, editors, Proceedings of the Fourth International Conference on Precision Agriculture, St. Paul, MN. 19–22 June 1998. ASA, CSSA, and SSSA, Madison, WI. p. 979–990.

Sudduth, K.A., N.R. Kitchen, D.F. Hughes, and S.T. Drummond. 1995. Electromagnetic induction sensing as an indicator of productivity on claypan soils. In: P.C. Robert, R.H. Rust, and W.E. Larson, editors, Proceedings of the Second International Conference on Site-specific Management for Agricultural Systems. ASA, CSSA, SSSA, Madison, WI. p. 671–681.

Telford, W.M., L.P. Geldart, R.E. Sheriff, and D.A. Keys. 1976. Applied geophysics. Cambridge Univ. Press, Cambridge, UK.

Thompson, S.K. 1992. Sampling. John Wiley and Sons, New York.

Tian, Y., G.J. Huffman, R.F. Adler, L. Tang, M. Sapiano, V. Maggioni, and H. Wu. 2013. Modeling errors in daily precipitation measurements: Additive or multiplicative? Geophys. Res. Lett. 40:2060–2065. doi:10.1002/grl.50320

Triantafilis, J., A.I. Huckel, and I.O.A. Odeh. 2003. Field-scale assessment of deep drainage risk. Irrig. Sci. 21(4):183–192.

Triantafilis, J., and F.A. Monteiro Santos. 2010. Resolving the spatial distribution of the true electrical conductivity with depth using EM38 and EM31 signal data and a laterally constrained inverse model. Aust. J. Soil Res. 48:434–446. doi:10.1071/SR09149

Urban, D.L. 2002. Tactical monitoring of landscapes. In: J. Liu and W.W. Taylor, editors, Integrating landscape ecology into natural resource management. Cambridge Univ. Press, Cambridge, UK. p. 294–311. doi:10.1017/CBO9780511613654.016

Urdanoz, V., and R. Aragüés. 2012. Comparison of Geonics EM38 and Dualem 1S electromagnetic induction sensors for the measurement of salinity and other soil properties. Soil Use Manage. 28:108–112. doi:10.1111/j.1475-2743.2011.00386.x

US Salinity Laboratory Staff. 1954. Diagnosis and improvement of saline and alkali soils. USDA Handb. 60. US Gov. Print. Office, Washington, DC. p. 1–160.

Valliant, R., A.H. Dorfman, and R.M. Royall. 2000. Finite population sampling and inference: A prediction approach. John Wiley and Sons, New York.

Van Groenigen, J.W., G. Pieters, and A. Stein. 2000. Optimizing spatial sampling for multivariate contamination in urban areas. Environmetrics 11:227–244. doi:10.1002/(SICI)1099-095X(200003/04)11:2<227::AID-ENV404>3.0.CO;2-#

Van Groenigen, J.W., W. Siderius, and A. Stein. 1999. Constrained optimisation of soil sampling for minimisation of the kriging variance. Geoderma 87:239–259. doi:10.1016/S0016-7061(98)00056-1

Van Zijl, G., P. Le Roux, and H. Smith. 2012. Rapid soil mapping under restrictive conditions in Tete, Mozambique. In: B. Minasny, B. Malone, and A.B. McBratney, editors, Digital soil assessments and beyond: Proceedings of the 5th global workshop on digital soil mapping, Sydney, Australia. CRC Press, Boca Raton, FL. p. 335–339. doi:10.1201/b12728-66

Viscarra Rossel, R., V. Adamchuk, K.A. Sudduth, N. Mckenzie, and C. Lobsey. 2011. Proximal soil sensing: An effective approach for soil measurements in space and time. Adv. Agron. 113:237–282.

Vitharana, U.W.A., T. Saey, L. Cockx, D. Simpson, H. Vermeersch, and M. Van Meirvenne. 2008. Upgrading a 1/20,000 soil map with an apparent electrical conductivity survey. Geoderma 148(1):107–112. doi:10.1016/j.geoderma.2008.09.013

Walter, J., E. Lück, A. Bauriegel, C. Richter, and J. Zeitz. 2015. Multi-scale analysis of electrical conductivity of peatlands for the assessment of peat properties. Eur. J. Soil Sci. 66(4):639–650. doi:10.1111/ejss.12251

Warrick, A.W., R. Zhang, M.K. El-Harris, and D.E. Myers. 1988. Direct comparisons between kriging and other interpolators. In: P.J. Wierenga and D. Bachelet, editors, Proceedings of the Conference on Validation of Flow and Transport Models for the Unsaturated Zone. New Mexico State University, Las Cruces, NM.

Weber, D.D., and E.J. Englund. 1992. Evaluation and comparison of spatial interpolators. Math. Geol. 24:381–391. doi:10.1007/BF00891270

Williams, B.G., and G.C. Baker. 1982. An electromagnetic induction technique for reconnaissance surveys of soil salinity hazards. Aust. J. Soil Res. 20:107–118. doi:10.1071/SR9820107

Williams, B.G., and D. Hoey. 1987. The use of electromagnetic induction to detect the spatial variability of the salt and clay contents of soils. Aust. J. Soil Res. 25:21–27. doi:10.1071/SR9870021

Wollenhaupt, N.C., R.P. Wolkowski, and M.K. Clayton. 1994. Mapping soil test phosphorus and potassium for variable-rate fertilizer application. J. Prod. Agric. 7:441–448. doi:10.2134/jpa1994.0441

Wu, W., W. Al-Shafie, A. Mhaimeed, F. Ziadat, V. Nangia, and W. Payne. 2014. Soil salinity mapping by multi-scale remote sensing in Mesopotamia, Iraq. IEEE J. Selected Topics Appl. Earth Observ. Remote Sens. 7:4442–4452.

Yao, R., J. Yang, X. Zhao, X. Chen, J. Han, X. Li, M. Liu, and H. Shao. 2012. A new soil sampling design in coastal saline region using EM38 and VQT method. Clean Soil Air Water 40:972–979.

Zhang, T., J. Qi, Y. Gao, Z. Ouyang, S. Zeng, and B. Zhao. 2015. Detecting soil salinity with MODIS time series VI data. Ecol. Indic. 52:480–489. doi:10.1016/j.ecolind.2015.01.004

Zimmerman, D., C. Pavlik, A. Ruggles, and M.P. Armstrong. 1999. An experimental comparison of ordinary and universal kriging and inverse distance weighting. Math. Geol. 31:375–390. doi:10.1023/A:1007586507433